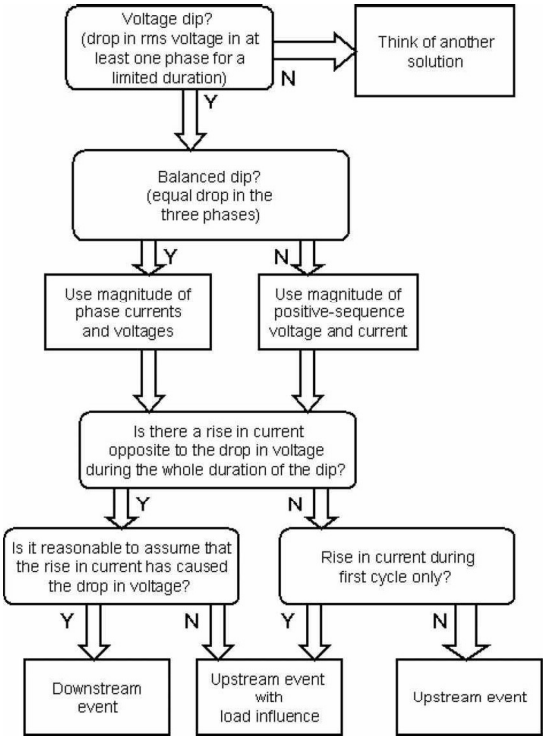


Figure 8.47 Algorithm for determining whether voltage dip has upstream or downstream origin.

and current rise corresponds with a reasonable value of the source impedance. A general algorithm is shown in Figure 8.47 that can be used to determine whether a voltage dip is due to an upstream or a downstream event.

8.10 TRANSIENTS

The characterization of transients in voltages is somewhat different from that of interruptions, swells, and sags. However, the general method in Figure 8.1 still applies here. The first choice to be made is the choice of "characteristic versus time". Two principally different approaches can be distinguished here:

- The original measured (sampled) waveform is used as a characteristic versus time.
- Characterization is based on the deviation from the normal waveform, that is, on the actual transient.

The choice of characterization method depends also on the way in which the transient is detected. In theory the detection method and the characterization

method are independent. For individual events any characterization method can be used, but especially when extracting statistics the characteristics should be related to the method used for detecting the event (the triggering method). When the triggering method and characteristics do not fit, the statistics may be irrelevant.

8.10.1 Extracting Transient Component

8.10.1.1 Test Signal To test the performance of methods for extracting the transient component a synthetic test signal has been created. The test signal consists of a double-frequency transient superimposed on a quasi-steady-state signal (a fundamental component with some minor harmonic distortion). The signal represents a typical voltage waveform. The random variations in the voltage during normal operation are included by using a random-walk model. The fundamental component at any sample instant is obtained from the value at the previous sample by adding a random number:

$$U_1(n+1) = U_1(n) + k(\rho - 0.5) \tag{8.55}$$

where ρ is a random sample from the uniform distribution on the interval (0,1). The result is a slow drift in the fundamental component. The same model was used for the third, fifth, and seventh harmonics. The amount of variation in the signal depends on the value of the constant k. For the fundamental component we have chosen $k = 0.096$ V, and for the harmonic components $k = 0.024$ V. The initial values were 230 V for the fundamental component and 5.75, 6.9, and 3.45 V (2.5, 3, and 1.5%) for harmonics 3, 5, and 7, respectively. From the fundamental and harmonic components as a function of time, the quasi-steady-state voltage waveform as a function of time has been calculated as follows:

$$\begin{aligned} U_s(t) = {} & U_1\sqrt{2}\sin(2\pi 50t) + U_3\sqrt{2}\sin(2\pi 150t) \\ & + U_5\sqrt{2}\sin(2\pi 250t) + U_7\sqrt{2}\sin(2\pi 350t) \end{aligned} \tag{8.56}$$

This signal is calculated over a window with a length of 14 cycles with a sampling frequency of 128 samples per cycle, resulting in a total of 1792 voltage values.

Added to this signal is a transient signal with a duration of two cycles, starting five cycles after the start of the quasi-steady-state signal. The transient signal consists of 370 and 410-Hz components with amplitudes of 23 and 12 V, respectively:

$$U_{\text{tr}}(t) = 23 \times \sqrt{2} \times \cos(2\pi 370t) - 12\sqrt{2}\cos(2\pi 410t) \tag{8.57}$$

The fundamental-voltage component further shows an increase of 8 V (2.5%) at the start of the transient. The total waveform is obtained by adding (8.56) and (8.57):

$$U(t) = U_s(t) + U_{\text{tr}}(t) \tag{8.58}$$

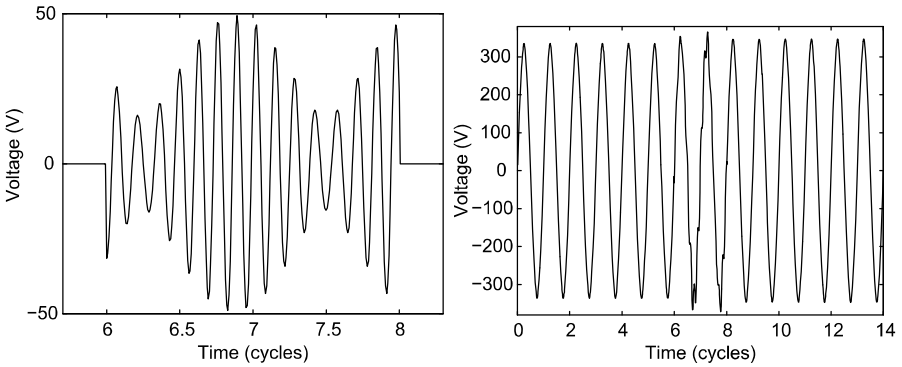


Figure 8.48 Synthetic transient (left) and total (right) signal used to test methods for extracting transient component.

The transient waveform, as in (8.57), and the total waveform, as in (8.58), are shown in Figure 8.48. This waveform will be used to test various methods for extracting the transient component from a measured waveform.

8.10.1.2 Cycle-by-Cycle Difference Comparing one cycle of the voltage or current waveform with the waveform one cycle earlier in time is a commonly used method to detect transients. This cycle-by-cycle difference could also be used for characterization purposes. One has to be careful, however, to prevent the same transient from coming back twice: One cycle after the transient there is again a difference with the previous cycle. One either has to limit the duration of the transient to less than one cycle or compare each cycle with the last cycle before the transient (alternatively the first cycle of the recording). The latter method has been used here.

The results of applying this method to the synthetic test signal are shown in Figure 8.49. The nonzero value before the event is due to the small variations in voltage between the first cycle (which has been used as a reference) and the sixth cycle (during which the transient occurred). The main difference between the original and extracted signals is however due to the change in the fundamental component. As the amplitude of the transient is at most 40 V, a change of 8 V in fundamental has a significant influence on the extracted transient.

To quantify the difference between the original and the extracted signal, and thus to quantify the performance of the extraction method, we define the rms error ε as follows:

$$\varepsilon = \sqrt{\frac{1}{N_2 - N_1} \sum_{N_1}^{N_2} (U_{\text{tr}} - U_{\text{xt}})^2} \tag{8.59}$$

with N_1 and N_2 the starting and ending points of the synthetic transient and U_{xt} the extracted signal, that is, the estimation of the original transient. The above calculations have been repeated 1000 times in order to get statistical information on the performance

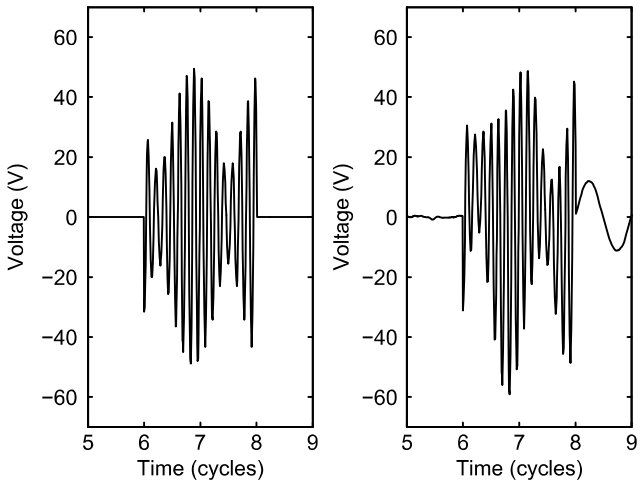


Figure 8.49 Original transient (left) and extracted transient (right).

of the algorithm. The resulting probability distribution function is shown in Figure 8.50. The majority of values are between 7 and 9 V; the mean value of the error, over all 1000 runs, is 8.0 V, and the standard deviation is 0.76 V.

It is no surprise that the expected rms error is close to 8 V as this is the contribution of the change in the fundamental component. As a comparison the distribution of the error has also been calculated in case there is no step in fundamental voltage. The results are shown on the right in Figure 8.50. The error is significantly less, with the majority of values between 0.5 and 1.5 V. The expected value and standard deviation are 0.85 and 0.42 V, respectively.

When applying the method to a measured waveform, another problem occurs: The length of one cycle is typically not equal to an integer number of samples. Comparing the signal value with the value one cycle back in time requires

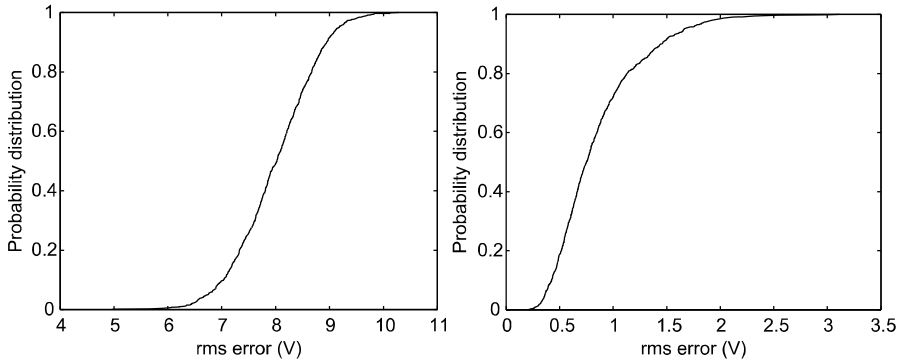


Figure 8.50 Distribution of rms error when extracting a transient by subtracting preevent waveform: with 8-V step in fundamental voltage (left); no step in fundamental (right).

interpolation between samples. This will make the implementation of the method more complicated. However, as a transient rarely lasts longer than a few cycles, the total error in the extracted transient will in many cases be dominated by the change in fundamental voltage associated with the transient.

8.10.1.3 Comparison with Average Fundamental Waveform Instead of comparing the measured waveform with the value one cycle back in time, the waveform can be compared with the fundamental waveform. This is easier to implement as there is no need for interpolation. When the extraction of the transient takes place in the monitor, a phase-locked loop may be used to generate the reference signal with which the waveform is compared.

This method has been applied to the same synthetic test signal as before. The original transient and the extracted transient are compared in Figure 8.51. When comparing with Figure 8.49 we see that even before the transient the difference signal is not fully zero. This is understandable as the harmonic distortion is not removed from the signal. The harmonic distortion thus becomes part of the extracted transient. After the transient, the extracted signal is a combination of the harmonic distortion and the change in fundamental. As the harmonic distortion is rarely less than a few percent of the fundamental, this will introduce a significant error in the extracted transient, especially for less severe transients.

This method has been tested by applying it to 1000 different synthetic signals, as for the previous method. The results are shown in Figure 8.52. The calculations have been performed for the case with an 8-V step in the fundamental and without a step in the fundamental. The error is about twice as large when there is a step in the fundamental. The expected rms errors are 9.03 and 4.27 V with and without a step in the

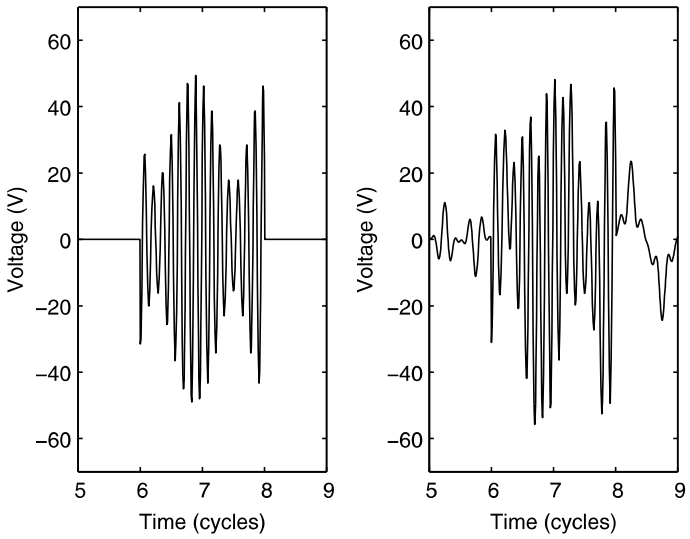


Figure 8.51 Original transient (left) and extracted transient (right).

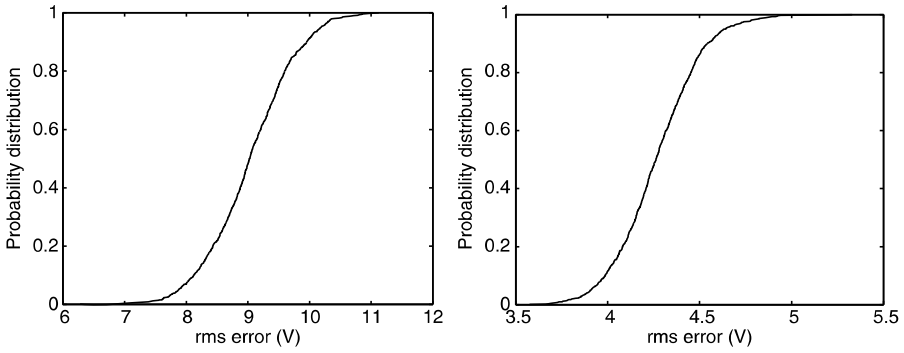


Figure 8.52 Distribution of rms error for synthetic signal with (left) and without (right) step in fundamental component.

fundamental, respectively. The standard deviations are 0.70 and 0.23 V, respectively. For both cases the error is bigger than for extracting the preevent waveform.

8.10.1.4 High-Pass Filter Output A straightforward way of removing the fundamental frequency is the use of a high-pass filter. The performance of the method depends to a large extent on the properties of the filter. The main aim of the filter is to remove the fundamental component, so that the stop band should include the power system frequency. Where possible also the dominant harmonics should be removed. The passband should include all the possible frequency components of the transient. As these are rarely known before, the choice of the stop-band edge and passband edge could be a problem. Capacitor-energizing transients as low as 250 Hz have been observed which would require a passband edge below 250 Hz. Unfortunately this will include the often dominant fifth- and seventh-harmonic components as well.

Where no lower frequency transients are present or expected, the passband edge should be around 300 to 400 Hz and the stop-band edge around 500 to 600 Hz. In case a passband edge of 250 Hz or lower has to be chosen, this method could be combined with the subtraction of the preevent waveform. In that case, the high-pass filter removes the fundamental component and the subtraction removes the harmonics. What remains are the changes in harmonic distortion associated with the transient.

This method has again been applied to the synthetic test signal. The results are shown in Figure 8.53. A type II Chebychev filter was chosen with a stop-band edge at 50 Hz. The left-hand figure has been obtained for a filter with passband edge at 250 Hz, passband ripple 0.1 dB, and stop-band attenuation 40 dB. For the right-hand filter the design criteria were passband edge 150 Hz, passband ripple 1 dB, and stop-band attenuation 80 dB.

The output of the signal before and after the transient is very similar; the steady-state output is slightly less for the one on the left due to the higher damping of the third-harmonic component. The initial oscillation is more severe in the first case. However, the initial oscillation can be easily handled by repeating the first cycle

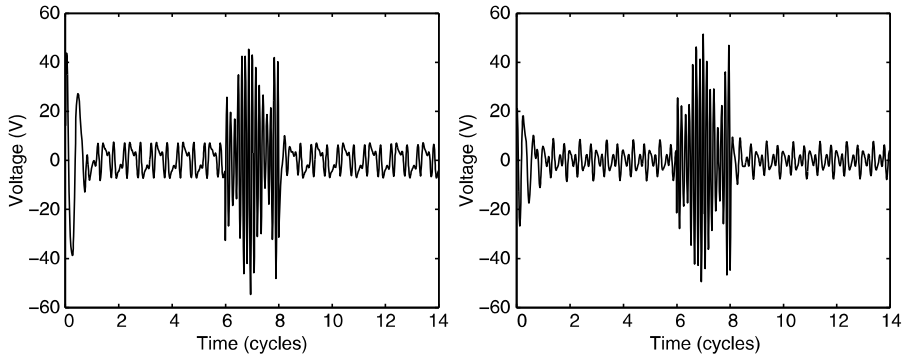


Figure 8.53 Transient extracted by high-pass filter from synthetic waveform: 150 Hz passband edge (left); 250 Hz passband edge (right).

of the recording a number of times so that the oscillation is damped out well before the actual transient starts. But when the transient is associated with a significant change in fundamental component (this is, e.g., the case for current measurements during downstream switching actions), a similar oscillation will appear due to this change in fundamental component.

A problem that may occur with any digital filter is the introduction of phase errors or *waveform distortion*. The sharper the transition between the stop band and pass-band, the higher the risk of phase errors. To show the impact of the phase error, the extracted waveform and the original transient are compared in detail in Figure 8.54 for the second example (250 Hz, 1.0 dB, 80 dB).

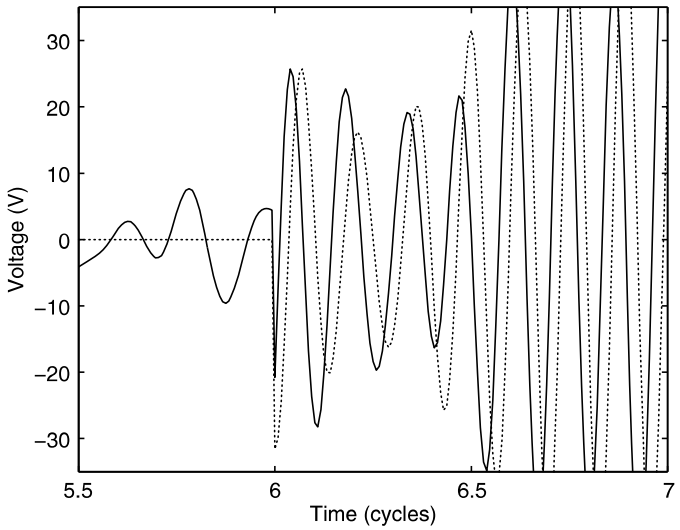


Figure 8.54 Comparison of high-pass-filter output (solid line) and original signal (dotted line).

TABLE 8.16 Performance of Different High-Pass Filters: Expected Value and Standard Deviation of rms Error When Extracting transient

Stop-band Edge (Hz)	Passband Edge (Hz)	Passband Ripple (dB)	Stop-Band Attenuation	Expected Value (V)	Standard Deviation (V)
50	150	0.1	80	6.08	0.14
50	150	0.1	40	6.77	0.13
50	250	0.1	80	7.60	0.11
50	250	0.1	40	6.40	0.13
50	250	1	40	5.55	0.13
50	250	1	80	6.88	0.12
50	150	1	40	6.41	0.12
50	150	1	80	7.60	0.11

Calculating the rms error for this filter in the same way as for the earlier methods would result in a rather large error. The error is however mainly due to the time delay introduced by the filter. As long as the extracted transient has the same shape and magnitude as the original transient, any delay should not be seen as an error. Therefore the extracted transient has been delayed by a number of samples before the rms error was calculated as in (8.59). Different delay times were chosen until the lowest expected value was obtained for the rms error. The results for a number of different high-pass filters are shown in Table 8.16. We can conclude from the table that the properties of the high-pass filter do not have any significant influence on the rms error. Compare this with the expected error of 8 V for subtracting the preevent waveform.

8.10.1.5 Output of Notch Filter An alternative filter to remove the fundamental component is a so-called notch filter. Such a filter is able to remove the fundamental frequency completely: The transfer function is zero for the center frequency of the filter.

A second-order digital notch filter is designed in [221, Section 7.2.2]. The design starts from a second-order analog notch filter with the following transfer function:

$$H_a(s) = \frac{s^2 + \Omega_0^2}{s^2 + B_w s + \Omega_0^2} \tag{8.60}$$

where $\Omega_0 = 2\pi f_0$, with f_0 the angular notch frequency, and $B_w = 2\pi f_w$, with f_w the 3-dB bandwidth. Using a bilinear transformation, the following transfer function for the digital function, in the z domain, is obtained:

$$G(z) = \frac{\frac{1}{2}(1+\alpha) - \beta(1+\alpha)z^{-1} + \frac{1}{2}(1+\alpha)z^{-2}}{1 - \beta(1+\alpha)z^{-1} + \alpha z^{-2}} \tag{8.61}$$

with

$$\alpha = \frac{1 - \tan\left(\frac{1}{2}b_w\right)}{1 + \tan\left(\frac{1}{2}b_w\right)} \tag{8.62}$$

and

$$\beta = \cos(\omega_0) \tag{8.63}$$

where $b_w = 2\pi f_w/f_s$ is the *normalized angular notch frequency* and $\omega_0 = 2\pi f_0/f_s$ the *normalized angular 3-dB bandwidth*.

A second-order notch filter centered around 50 Hz with a 3-dB bandwidth of 20 Hz has been used to extract the transient. The results are shown in Figure 8.55 for the same synthetic signal used before. In right-hand figure, the original transient is shown as a dotted line. The difference between the extracted transient and the actual transient is almost exclusively due to the harmonic distortion which is not removed by the filter. But just like the high-pass filter the output of the notch filter shows oscillations for a change in fundamental and at the start of the transients. The oscillations at the start of the signal are significant: with an amplitude of 75% of the step in fundamental and they take about four cycles to decay. This could be a problem for transients associated with a large change in the fundamental component.

The initial oscillation can be reduced by increasing the bandwidth of the filter. This however leads to a larger error in amplitude and phase angle. The performance of the notch filter, expressed as an expected rms error, has been calculated as a function of the 3-dB bandwidth. The result is shown in Figure 8.56. Each point is the average of 1000 stochastically independent runs. The standard deviation is small however (around 0.13 V for most values of the bandwidth); the error is mainly due to the distortion in the waveform. The rms error has been calculated for a delay of two samples and one sample and for no delay; the lowest rms error has been chosen for the curve. The minimum around 150 Hz corresponds to a time

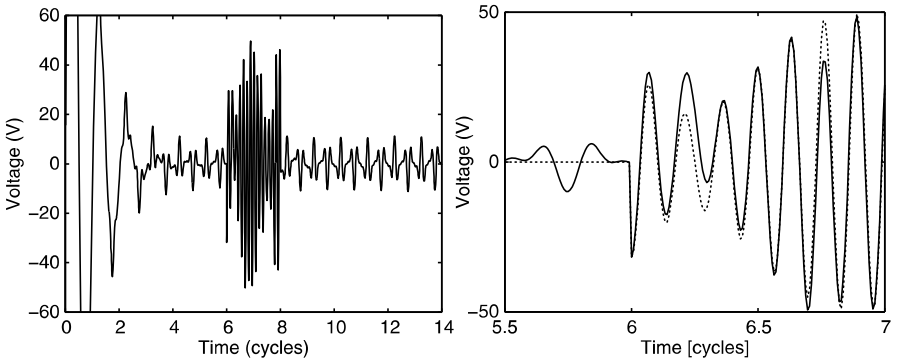


Figure 8.55 Transient extracted by notch filter from synthetic waveform; 20-Hz bandwidth.

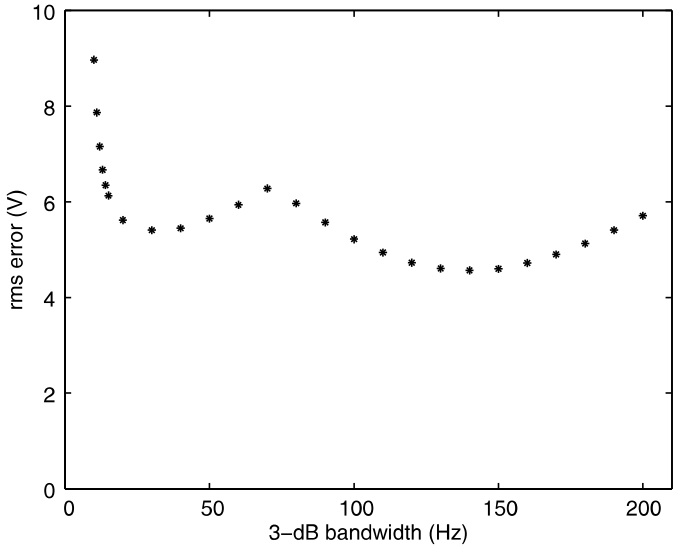


Figure 8.56 Expected rms error for notch filters with different bandwidth.

shift between input and output of the filter of close to one sample. At 70 Hz bandwidth the error is the same for no delay and one-cycle delay. For a bandwidth less than 30 Hz, the oscillations due to the step in fundamental start to affect the result. This explains the steep rise in rms error for smaller bandwidths.

8.10.2 Transients: Single-Event Indices

The characterization of transients is in most cases based on magnitude and duration: the same two terms used for voltage dips. However, the terms have a different definition than for voltage dips. The use of the same terminology means that dips and transients are sometimes plotted in the same magnitude–duration curve. The standard example is the CBEMA curve [33, Section 5.2.4], where the time scale ranges from less than 1 ms through several seconds. The shortest duration of a voltage dip is 10 ms; the short-duration part of the curve refers to transients. Although the use of the curve is mathematically incorrect, it remains a very useful tool for presenting a wide range of power quality events.

The main problem, however, is not the presentation of dips and transients in one curve but the difficulties in defining the magnitude and duration of transients. A number of different methods exist that lead to significantly different results. We will discuss a number of methods below, including some of their advantages and disadvantages. The choice of method to use will depend among others on the application. When characterizing the performance of the supply, it is in general recommended to use a number of different methods so as to maximize the application range.

The method for determining the single-event indices is determined from the characteristics versus time, which are in the case of transients either the original waveform or the extracted transients by using any of the methods discussed in Section 8.10.1. We will introduce a number of methods below, present the problems in definition, and apply the method to a number of measurement examples.

8.10.2.1 Peak Value A simple method of characterizing a transient is by its highest absolute value. A distinction may be made between the positive and the negative peaks when more detail is required. The main disadvantage of this method is that its result may strongly depend on the bandwidth of the measurement equipment. For very fast transients, the transient amplitude gets lower for a smaller bandwidth. As a rule of thumb, if the peak value is far outside the range of the other values, the actual peak value is likely to have been much higher. Such a recording may still have its value for trouble shooting purposes and for understanding the power system behavior, but it should not be used for characterization purposes. For pulses with a short rise time the peak value is also very much affected by the anti-aliasing filter. We will study the effect of the anti-aliasing filter in the next section. Some monitors contain a special (often mainly analoge) circuit to detect the peak value of voltage and current transients.

An advantage of using the peak value as a single-event index is that it is not affected by the setting of a threshold. Most of the indices discussed below are affected in different ways.

The resulting peak value depends strongly on whether the actual waveform is considered or only the extracted transient. The peak value has been calculated for three examples. The same examples will be used for the other single-event indices. For each example only one phase has been considered. The first example is an impulsive transient in the current. The actual waveform and the extracted transient are shown in Figure 8.57. A notch filter with a bandwidth of 30 Hz has been used to extract the transient.

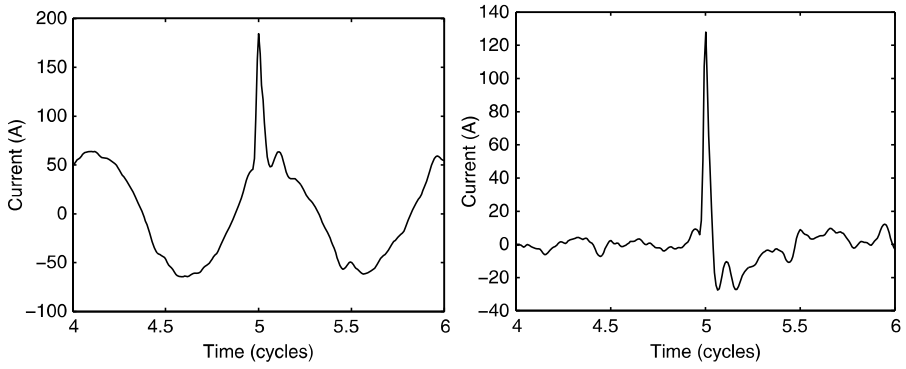


Figure 8.57 Impulsive current transient: original waveform (left) and extracted transient (right).

The highest absolute value of the original waveform is 184 A; the highest absolute value of the extracted transient is 128 A. In this case the difference between these two values (56 A) is close to the amplitude of the preevent waveform (65 A). Note, however, that this only holds for transients near the maximum or minimum of the steady-state waveform. Also the initial direction of the transient should correspond with the sign of the steady-state waveform. We will see from the forthcoming examples that there is no general relation between the peak of the original waveform and the peak of the extracted transient.

The peak value can be expressed in a number of different ways, each leading to a different result. Some examples are given below, together with the resulting values. When quoting a value for any single-event index it is always very important to indicate how this value has been calculated. Future standards may simplify this by prescribing the way to calculate the indices. In the list below, I_p is the highest absolute value of the original waveform, $I_{\mathrm{tr},p}$ the highest absolute value of the extracted transient, $I_{\mathrm{ss},p}$ the highest absolute value of the steady-state (preevent) waveform, and I_{nom} the (rms value of the) nominal current. For the calculation we assumed a nominal current of 55 A.

- The peak of the original waveform, $I_p = 184$ A.
- The absolute overshoot of the original waveform compared to the preevent waveform, $I_p - I_{\mathrm{ss},p} = 119$ A.
- The absolute overshoot of the original waveform compared to the nominal waveform, $I_p - \sqrt{2}I_{\mathrm{nom}} = 106$ A.
- The relative peak of the original waveform compared to the preevent waveform, $I_p/I_{\mathrm{ss},p} = 283\%$.
- The relative overshoot of the original waveform compared to the preevent waveform, $(I_p - I_{ss,\mathrm{p}})/I_{ss,\mathrm{p}} = 183\%$.
- The relative peak of the original waveform compared to the nominal waveform, $I_p/\sqrt{2}\, I_{\mathrm{nom}} = 236\%$.
- The relative overshoot of the original waveform compared to the preevent waveform, $(I_p - I_{\mathrm{nom}})/I_{\mathrm{nom}} = 136\%$.
- The peak of the extracted transient, $I_{\mathrm{tr},p} = 128$ A.
- The relative peak of the extracted transient compared to the preevent waveform, $I_{\mathrm{tr},p}/I_{\mathrm{ss},p} = 197\%$.
- The relative peak of the extracted transient compared to the nominal waveform, $I_{\mathrm{tr},p}/\sqrt{2}I_{\mathrm{nom}} = 165\%$.

The second example is an oscillatory transient due to capacitor energizing: measured in a 60-Hz, 120-V system. The original waveform and the extracted transient are shown in Figure 8.58. The figure shows a typical capacitor-energizing transient, with a first step in voltage toward zero (i.e., in opposite direction to the sign of the voltage), followed by an exponentially damped oscillation. The oscillation is especially clear in the extracted transient. Also note that the oscillation is of rather low frequency, about 300 Hz in this case.

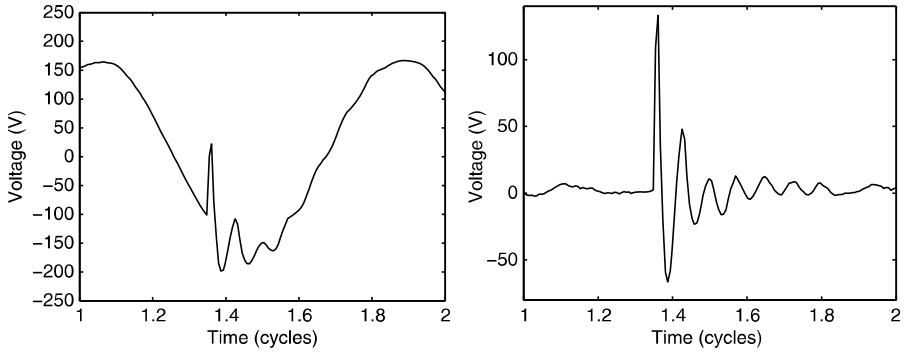


Figure 8.58 Oscillatory voltage transient: original waveform (left); extracted transient (right).

The following peak values are obtained for this transient:

- The peak of the original waveform, $U_p = 199$ V.
- The relative overshoot of the original waveform compared to the preevent waveform, $(U_p - U_{\mathrm{ss},p})/U_{\mathrm{ss},p} = 21\%$.
- The peak of the extracted transient, $U_{\mathrm{tr},p} = 133$ V.
- The relative peak of the extracted transient compared to the preevent waveform, $U_{\mathrm{tr},p}/U_{\mathrm{ss},p} = 81\%$.

For voltages the preevent peak is close to the nominal peak, so there is no need to distinguish between them. Note that the overvoltage in the original waveform is only 21%, despite the peak of the extracted transient being 81% of the steady-state peak.

The third example is shown in Figure 8.59: an oscillatory voltage transient measured in a 10-kV, 50-Hz system. The transient is associated with a drop in rms voltage of about 1.5%. Using the relation between voltage step and resonance

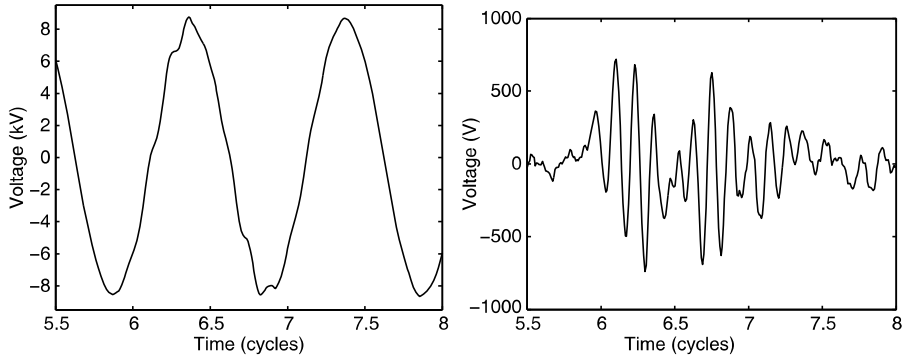


Figure 8.59 Double-frequency oscillatory voltage transient: original waveform (left); extracted transient (right).

frequency for capacitor energizing, this would correspond to an oscillation frequency of about 400 Hz, which is in agreement with the measurement. The extracted transient is of a different character than the one shown in Figure 8.58. This is due to the presence of a second oscillation frequency. The modulation frequency of the amplitude of the oscillation equals the difference frequency, about 80 Hz in this case. A likely explanation for this transient is restrike during capacitor deenergizing at the next voltage level (132 kV), which excites a double-frequency oscillation together with the capacitor at the local 10-kV bus.

The peak of the extracted transient is 740 V, 8.5% of the steady-state peak. The original transient shows almost no overvoltage, only 0.5%. Without extracting the transient, this event would have been very difficult to detect.

8.10.2.2 Impact of Filtering on Peak Value When a short-duration pulse appears at the terminals of a monitor, its high-frequency components will be removed by the anti-aliasing filter. This will typically lead to a reduction in the amplitude (peak value) of the pulse. Sampling takes place after the anti-aliasing filter, so that the peak value as obtained by the processing of the digital waveform is not a good estimation for the peak value of the actual waveform.

As an example we consider a monitor using a sampling rate of 12.8 kHz (256 samples per cycle in a 50-Hz system). We choose a passband edge at 3 kHz and the corresponding stop-band edge at 9.8 kHz. (See Section 3.2.3 for a discussion of the design criteria for anti-aliasing filters.) These requirements are met by an analog Butterworth filter of order 7 and natural frequency 4300 Hz.

Test pulses were created with a zero rise time and decay time constants of 70 and 350 μs. The test pulses were applied to the above-mentioned anti-aliasing filter. The results are shown in Figure 8.60, where the solid line gives the test waveform and the dotted line the output of the anti-aliasing filter. We see that the filter causes a significant drop in peak voltage as well as a delay of about 0.3 ms. Note that both input and output of the anti-aliasing filter are analog signals; sampling takes place after the

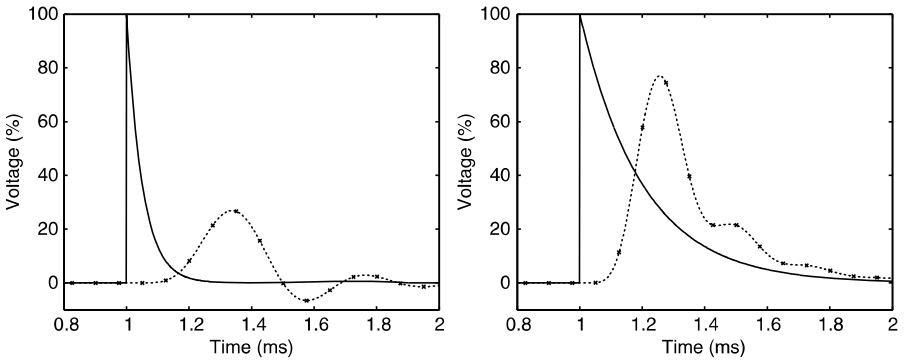


Figure 8.60 Input pulse (solid) and output (dotted) of anti-aliasing filter with sampled waveform (crosses). Left: 70 μs time constant; right: 350 μs time constant.

anti-aliasing filter. The crosses indicate the sampled waveform. Note that the position of the first sample can be taken at random. This implies that there is some uncertainly in the highest value of the sampled waveform. If a sample instant corresponds with the peak of the analog waveform, the highest value of the sampled waveform is about 27% in this example. But if the peak of the analog waveform comes just between two sampling instants, the observed peak value is about 25%.

The peak value as observed by the monitor depends on the time constant of the original impulse. This effect is quantified in Figure 8.61, where the peak value after the anti-aliasing filter is shown as a function of the time constant of the impulse. The time constant has been varied between 10 and 500 μs to represent overvoltages due to lightning strokes. (See [146] for a discussion of the range of time constants of lightning strokes.) As we can see in Figure 8.60, the shape of the waveform around the peak is not affected by the time constant. There are some differences in the tail of the signal, but these will be hard to detect as the transient is superimposed on a distorted steady-state signal. When using the peak voltage to quantify impulsive transients, care should be taken that the bandwidth of the complete measurement chain is sufficiently wide.

When using the extracted transient to determine the peak value, it is further important to choose the filter parameters in an appropriate way. We saw before that the choice of filter and its parameter values affect the waveform of the extracted transient. To illustrate this, the impact of the bandwidth for a notch filter on the estimated peak value has been determined. The results are shown in Figure 8.62 for the impulsive current transient shown in Figure 8.57. We see a steady decrease of the peak value with increasing bandwidth. The larger the bandwidth, the more the higher frequencies are affected, so that a low bandwidth would be preferable.

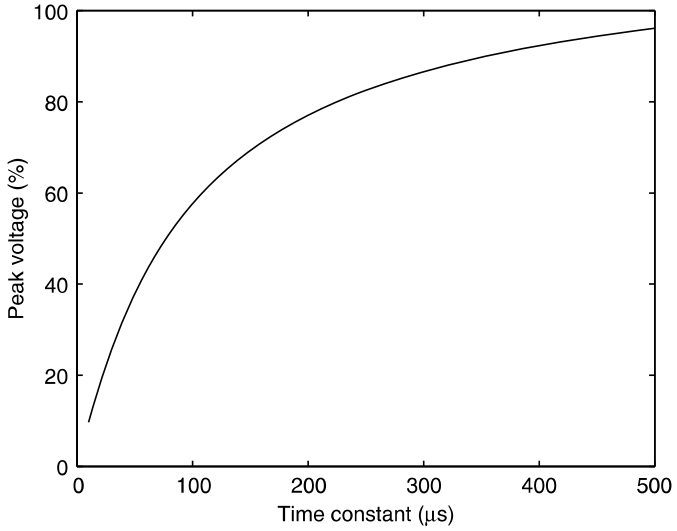


Figure 8.61 Attenuation of peak of impulsive transient by anti-aliasing filter.

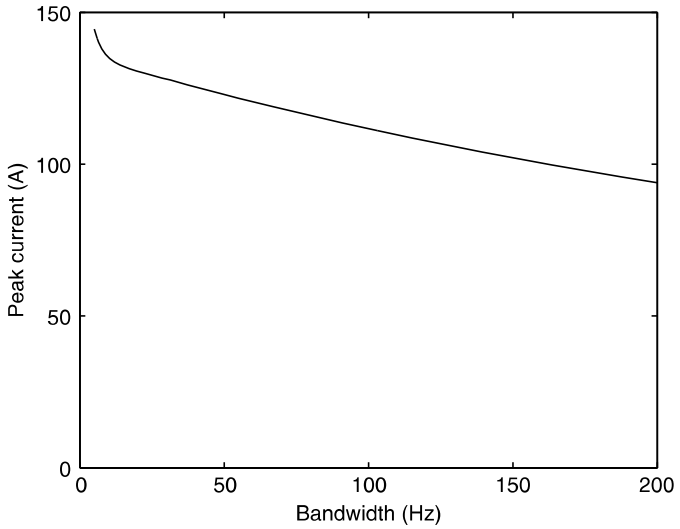


Figure 8.62 Impact of notch filter bandwidth on estimated peak value of extracted transient.

However, for a bandwidth less than about 20 Hz, the change in steady state associated with the transient causes additional oscillations at the output of the notch filter. This results in an apparent increase in peak value.

8.10.2.3 Duration The duration of a transient can be defined in a number of ways. However, the most appropriate way is to define the duration of a transient as the amount of time during which the voltage or current is above a threshold. This method is very similar to the method used for defining the duration of dips, swells, and interruptions. The more complicated character of transients requires however a number of additional issues to be defined:

- The absolute value of voltage or current should be compared with the threshold level.
- Either the original waveform or any of the methods to obtain the extracted transient can be used to determine the duration of the event. Obviously the choice of waveform compared with the threshold affects the resulting value.
- For oscillating transients (the majority of transients), multiple threshold crossings may occur, especially when the extracted transient is used. The duration should be defined as the time between the first upward threshold crossing and the last downward threshold crossing.

The main problem in quantifying the duration of a transient is the choice of the threshold. As the duration is defined as the time above threshold, the threshold level will affect the value of the duration. The higher the threshold level, the lower the resulting value for the duration. A suitable choice for the threshold used

for calculating the duration would be the same threshold as the one used for detecting the transient. This is especially recommended when the single-event indices are used to obtain statistics.

To show how the choice of threshold affects the apparent duration of the event, the impulsive current transient shown in Figure 8.57 is plotted again in Figure 8.63. The absolute value of both the original waveform and the extracted transient are shown, together with a number of suitable threshold levels. The threshold levels for the original waveform correspond to 110, 120, and 130% of the nominal peak current ($\sqrt{2} \times 55$ A in this case). The crosses indicate the actual voltage samples; the duration equals the time step (0.1563 ms in this case) times the number of sampled voltages above the threshold. A threshold setting equal to 110% of the nominal peak corresponds to the common setting used for detection of swells: 110% of nominal rms voltage. The resulting duration is 1.09 ms. The same value of the duration would be obtained for a 120% threshold setting; for a 130% threshold the duration becomes 0.78 ms.

The threshold setting has more impact when the extracted transient is used, as shown in the right-hand plot in Figure 8.63. The threshold setting of 10% would somewhat correspond to a 110% threshold for the original waveform. However, the harmonic distortion after the event results in a steady-state high-pass component with an amplitude exceeding 10%. Such a severe distortion is uncommon for voltage waveforms but occurs occasionally for current waveforms, especially measurements close to distorting equipment. In this case a 10% threshold setting would lead to an infinite duration of the threshold. But even for a 20 or 30% threshold setting determining the duration is not straightforward. What looks like an impulsive transient in the original waveform turns out to be an oscillatory transient from the extracted transient. This is rather common; pure impulsive transients are very rare. The result of the oscillatory character of the event is that the threshold is crossed multiple times. In this case, where the transient is dominated by the first peak, the duration could be defined as the time between the first upward and the first downward threshold crossing. We will soon see examples where such a definition makes no sense.

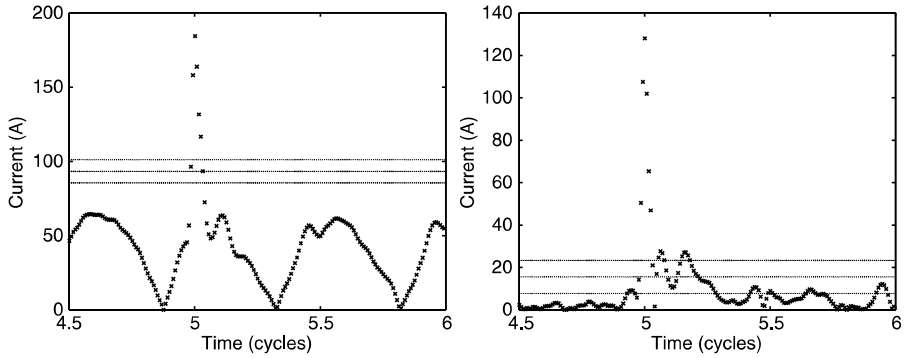


Figure 8.63 Absolute value of original waveform (left) and of extracted transient (right) compared with a number of thresholds (dotted lines); waveform in Figure 8.57.

TABLE 8.17 Duration for Different Threshold Settings and Different Duration Definitions: Impulsive Current Transient

Threshold Setting	20/120% (ms)	30/130% (ms)
Original waveform	1.09	0.78
Extracted transient		
First downward to first upward zero crossing	1.09	0.94
First downward to last upward zero crossing	4.69	4.06
Total time above threshold	3.75	2.34

Instead the duration should be defined either as the time between the first upward and the last downward threshold crossing or as the total time above threshold. The values resulting from the three different definitions are summarized in Table 8.17 for two threshold settings. We again see that it is very important to clearly define the way in which the index is defined. The resulting duration varies from less than 1 ms up to almost 5 ms, even for a simple transient.

The second example is the oscillatory voltage transient due to capacitor energizing, as shown in Figure 8.58. The absolute value of the voltage waveform and the extracted transient are shown in Figure 8.64. The thresholds are given for the same percentage values as before: 10/110, 20/120, and 30/130% of the nominal voltage of 120 V. The first observation is that the original waveform only just exceeds the 110% threshold. Setting the threshold to 120% of nominal or higher would lead to missing the threshold when the original transient would be used for detection. The extracted transient on the right exceeds even the 30% threshold without any problem.

The resulting duration values are shown in Table 8.18 together with the values for other single-event indices, to be discussed below.

The transient in the third example (Figure 8.59) has a very small amplitude compared to the steady-state signal. This means that the output of the notch filter will be

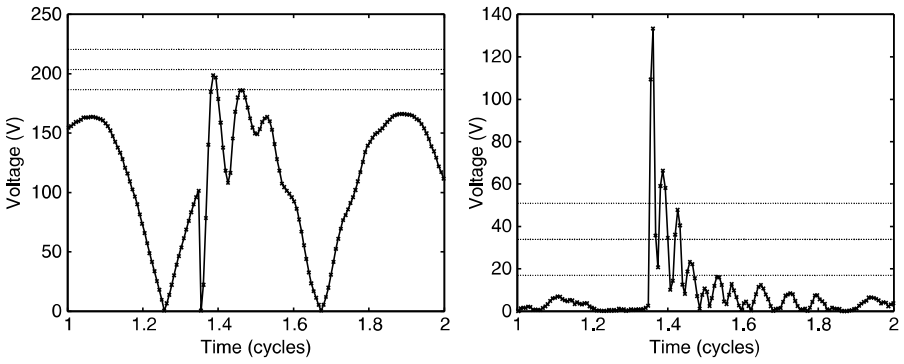


Figure 8.64 Absolute value of original waveform (left) and of extracted transient (right) compared with a number of thresholds (dotted lines); waveform in Figure 8.58.

TABLE 8.18 Overview of Single-Event Indices for Transient in Figure 8.64 at Threshold Settings of 10, 20, and 30%

	Duration (ms)			V_t Integral (ms V)			Transient energy (V^2s)		
Duration Definition	10%	20%	30%	10%	20%	30%	10%	20%	30%
Time between first upward and last downward zero crossing	2.34	1.69	0.91	98.2	87.1	63.2	6.65	6.44	5.56
Total time above threshold	1.82	1.30	0.65	91.9	80.9	55.5	6.58	6.34	5.34

dominated by harmonic components. The absolute value of the extracted transient is plotted in Figure 8.65 together with thresholds of 3% and 5% of the steady-state peak. It is clear that this event is close to the detection limit for this method (i.e., using the output of a notch filter). Subtracting the preevent waveform may do slightly better in this case, but even for that method a threshold less than 2% will cause difficulties due to the 1.5% drop in rms voltage associated with the transient. The double-frequency character further means that the beginning and end of the transient are difficult to detect. The result is that the apparent duration depends very much on the threshold setting. The impact on the V_t integral and transient energy is less.

The single-event indices are given in Table 8.19 for threshold settings of 3 and 5% of the steady-state peak, corresponding to the two lines in Figure 8.65. We see that the transient energy is again the least affected by the threshold setting

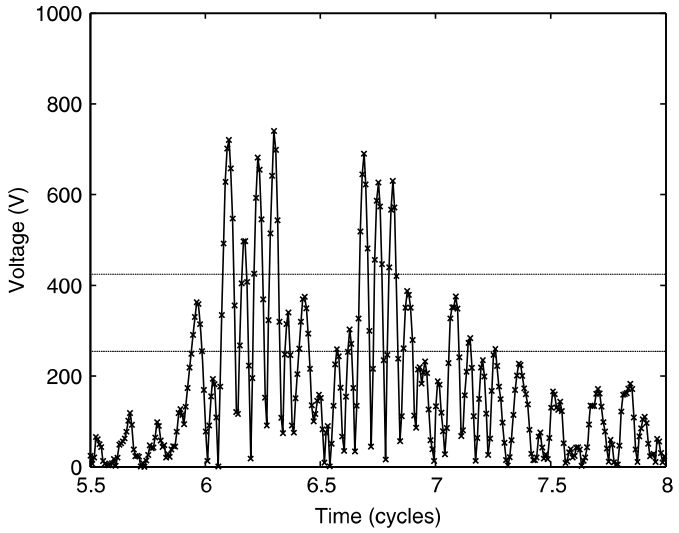


Figure 8.65 Absolute value of extracted transient compared with a number of thresholds (dotted lines); waveform in Figure 8.59.

TABLE 8.19 Overview of Single-Event Indices for Transient in Figure 8.59 at Threshold Settings of 3 and 5%

	Duration (ms)		V_t Integral (V s)		Transient energy (V^2 s)	
Duration Definition	3%	5%	3%	5%	3%	5%
Time between first upward and last downward zero crossing	26.4	15.0	7.1	4.9	2810	2249
Total time above threshold	11.5	5.0	5.1	2.9	2453	1734

and the integration window. The ratios between the highest and lowest values are 5.3 for the duration, 2.4 for the V_t integral, but only 1.6 for the transient energy.

8.10.2.4 V_t Integral Due to the problems in determining the peak value, an integration of the voltage or current over the duration of the event is used to characterize the severity of the transient. The V_t integral is defined as

$$V_t = \int_0^T v(t)\,dt \tag{8.64}$$

In case of current transients the I_t integral is defined in the same way. When using the V_t or I_t integral it is important to define the window over which the integral is taken. The most obvious choice is to take the integral over the time during which the voltage or current is above the threshold. In that case, the threshold level affects the value of the integral. This should be considered when comparing surveys: The setting of the threshold affects both the duration and the integral of the event. The lower the threshold, the longer the duration and the higher the integral; in other words, the severity of the event appears to increase with a reduction of the threshold. The resulting values for the impulsive current transient are summarized in Table 8.20.

From the duration and the V_t integral it is possible to calculate an equivalent voltage:

$$V_{\text{eq}} = \frac{V_t}{T} \tag{8.65}$$

TABLE 8.20 I_t Integral for Different Threshold Settings and Different Duration Definitions: Impulsive Current Transient, Figure 8.57

Duration Definition	20/120% (mA s)	30/130% (mA s)
Original waveform	156.5	133.0
Extracted transient		
First upward to first downward zero crossing	83.7	80.4
First upward to last downward zero crossing	152.5	141.2
Total time above threshold	140.5	114.3

TABLE 8.21 Average Current for Different Threshold Settings and Different Duration Definitions: Impulsive Current Transient, Figure 8.57

Duration Definition	20/120% (A)	30/130% (A)
Original waveform	144	171
Extracted transient		
First upward to first downward zero crossing	77	86
First upward to last downward zero crossing	33	35
Total time above threshold	37	52

This value is equal to the average voltage during the integration period. An increase in threshold will thus result in an increase in equivalent voltage. The equivalent current can be calculated in the same way for a current transient. The results for the impulsive current transient are shown in Table 8.21, again for two values of the threshold setting: 20% and 30% of nominal peak.

8.10.2.5 Transient Energy An alternative definition for the severity of the transient is the so-called 'transient energy'. The transient energy is defined as

$$E = \int_0^T v^2(t)\,dt \tag{8.66}$$

The transient energy, when calculated from the original waveform, is a measure of the amount of energy absorbed by equipment due to an overvoltage. The overvoltage part of the well-known CBEMA curve [33, Section 5.2.4] is based on the fact that equipment can absorb a certain amount of transient energy. Also the performance of fuses and current-limiting circuit breakers is based on the transient energy of the fault current through the interrupting device. This method has again been applied to the impulsive current transient, with the results summarized in Table 8.22.

TABLE 8.22 Transient Energy for Different Threshold Settings and Different Duration Definitions: Impulsive Current Transient, Figure 8.57

Duration Definition	20/120% (A^2 s)	30/130% (A^2 s)
Original waveform	21.6	19.7
Extracted transient		
First upward to first downward zero crossing	7.5	7.4
First upward to last downward zero crossing	9.0	8.8
Total time above threshold	8.8	8.3

8.10.3 Transients in Three Phases

Most power quality measurements take place in three-phase systems. A voltage or current transient rarely affects only one phase, so a three-phase approach is needed to fully understand the event. The event can be studied by comparing the transients in the respective phases. An alternative approach will be developed here. The approach is similar to the classification of three-phase unbalanced voltage dips, as discussed in Section 6.2.3.

8.10.3.1 Theory The start of the method is the so-called Clarke transform as introduced by E. Clarke [68] to simplify calculations of traveling waves along overhead transmission lines. The method is discussed among others in [279, Section 5.4; 320, Section 6.2.1]. The Clarke transform relates phase voltages and component voltages through the following matrix expression:

$$\begin{pmatrix} V_a \\ V_b \\ V_c \end{pmatrix} = \begin{bmatrix} -1 & 0 & 1 \\ -\frac{1}{2} & \frac{1}{2}\sqrt{3} & 1 \\ -\frac{1}{2} & -\frac{1}{2}\sqrt{3} & 1 \end{bmatrix} \begin{pmatrix} V_\alpha \\ V_\beta \\ V_0 \end{pmatrix} \tag{8.67}$$

The components are referred to as the *alpha component*, *beta component* and *zero-sequence component*. The advantage of this method over the symmetrical-component transformation is that the transformation matrix only contains real elements. This makes it possible to do the transformation in the time domain.

The alpha component gives a voltage in phase a and the opposite voltage of half the amplitude in phases b and c. [Fill in $V_\alpha = 1$, $V_\beta = 0$, $V_0 = 0$ in (8.67).] This corresponds to the type Da dip that was introduced in Tables 6.2 and 6.4. The beta-component gives a voltage in phase b and the opposite voltage in phase c. This corresponds to a type Ca dip. The zero-sequence component results in the same voltage in the three phases.

Note that expressions for the voltage dips in three phases were given for the residual complex voltages. With transients, however, we are interested in the changes compared to the preevent voltages. Rewriting the expressions for dip types C and D in terms of changes in complex voltage results for type D in

$$\begin{aligned} \Delta U_a &= E - V \\ \Delta U_b &= -\tfrac{1}{2}(E - V) \\ \Delta U_c &= -\tfrac{1}{2}(E - V) \end{aligned} \tag{8.68}$$

and for type C in

$$\begin{aligned}\Delta U_a &= 0\\ \Delta U_b &= +\tfrac{1}{2}j(E-V)\sqrt{3}\\ \Delta U_c &= -\tfrac{1}{2}j(E-V)\sqrt{3}\end{aligned} \tag{8.69}$$

Substituting $V_\alpha = E - V$ in (8.68) and $V_\beta = j(E - V)$ in (8.69) results in (8.67).

To calculate the component voltages from the phase voltages, the inverse transformation of (8.69) is needed:

$$\begin{pmatrix} V_\alpha \\ V_\beta \\ V_0 \end{pmatrix} = \frac{1}{3}\begin{bmatrix} 2 & -1 & -1 \\ 0 & \sqrt{3} & -\sqrt{3} \\ 1 & 1 & 1 \end{bmatrix}\begin{pmatrix} V_a \\ V_b \\ V_c \end{pmatrix} \tag{8.70}$$

We may thus refer to the alpha and beta components as the Da and Ca components, respectively. The other dip types are obtained by cyclic rotation of (8.67);

$$\begin{pmatrix} V_a \\ V_b \\ V_c \end{pmatrix} = \begin{bmatrix} -\frac{1}{2} & -\frac{1}{2}\sqrt{3} & 1 \\ 1 & 0 & 1 \\ -\frac{1}{2} & -\frac{1}{2}\sqrt{3} & 1 \end{bmatrix}\begin{pmatrix} V_{\mathrm{Db}} \\ V_{\mathrm{Cb}} \\ V_0 \end{pmatrix} \tag{8.71}$$

with as inverse transformation

$$\begin{pmatrix} V_{\mathrm{Db}} \\ V_{\mathrm{Cb}} \\ V_0 \end{pmatrix} = \frac{1}{3}\begin{bmatrix} -1 & 2 & -1 \\ -\sqrt{3} & 0 & \sqrt{3} \\ 1 & 1 & 1 \end{bmatrix}\begin{pmatrix} V_a \\ V_b \\ V_c \end{pmatrix} \tag{8.72}$$

and for the Dc and Cc components

$$\begin{pmatrix} V_a \\ V_b \\ V_c \end{pmatrix} = \begin{bmatrix} -\frac{1}{2} & \frac{1}{2}\sqrt{3} & 1 \\ -\frac{1}{2} & -\frac{1}{2}\sqrt{3} & 1 \\ 1 & 0 & 1 \end{bmatrix}\begin{pmatrix} V_{\mathrm{Dc}} \\ V_{\mathrm{Cc}} \\ V_0 \end{pmatrix} \tag{8.73}$$

with as inverse transformation

$$\begin{pmatrix} V_{\mathrm{Dc}} \\ V_{\mathrm{Cc}} \\ V_0 \end{pmatrix} = \frac{1}{3}\begin{bmatrix} -1 & -1 & 2 \\ \sqrt{3} & -\sqrt{3} & 0 \\ 1 & 1 & 1 \end{bmatrix}\begin{pmatrix} V_a \\ V_b \\ V_c \end{pmatrix} \tag{8.74}$$

Note that the zero-sequence component is the same in all three cases, so only seven different components result. All seven components can be obtained from the phase voltages by combining (8.70), (8.72), and (8.74), resulting in the following matrix expression:

$$\begin{pmatrix} V_{\mathrm{Da}} \\ V_{\mathrm{Db}} \\ V_{\mathrm{Dc}} \\ V_{\mathrm{Ca}} \\ V_{\mathrm{Cb}} \\ V_{\mathrm{Cc}} \\ V_0 \end{pmatrix} = \frac{1}{3}\begin{bmatrix} 2 & -1 & -1 \\ -1 & 2 & -1 \\ -1 & -1 & 2 \\ 0 & \sqrt{3} & -\sqrt{3} \\ -\sqrt{3} & 0 & \sqrt{3} \\ \sqrt{3} & -\sqrt{3} & 0 \\ 1 & 1 & 1 \end{bmatrix}\begin{pmatrix} V_a \\ V_b \\ V_c \end{pmatrix} \tag{8.75}$$

At this stage it is very important to realize that this is not the standard decomposition into orthogonal modal components: These seven components are not mutually independent; there will be cross-coupling between the components. Consider, for example, a Da-type transient: $V_\alpha = V_{\mathrm{Da}} = 1$, $V_\beta = V_{\mathrm{Ca}} = 0$, $V_0 = 0$ in (8.67). This results, after calculating the phase voltages from (8.67) and substituting these into (8.75), in the following values for the seven components:

$$\begin{aligned} V_{\mathrm{Da}} &= 1 \\ V_{\mathrm{Db}} &= -\tfrac{1}{2} \\ V_{\mathrm{Dc}} &= -\tfrac{1}{2} \\ V_{\mathrm{Ca}} &= 0 \\ V_{\mathrm{Cb}} &= -\tfrac{1}{2}\sqrt{3} \\ V_{\mathrm{Cc}} &= \tfrac{1}{2}\sqrt{3} \\ V_0 &= 0 \end{aligned} \tag{8.76}$$

The Da component is the dominating component but four other components also have a nonzero value. Only the Ca and zero-sequence components are zero: Da, Ca, and V_0 form an orthogonal base. The consequence of the choice to use seven components is that there will be multiple solutions: After all there are only three phase voltages,

which can be reproduced in an infinite number of ways from seven components. The aim is to reproduce a measured transient with the minimum number of components.

The cross-coupling between the seven components is given in the cross-coupling matrix:

$$\begin{pmatrix} V_{\mathrm{Da}} \\ V_{\mathrm{Db}} \\ V_{\mathrm{Dc}} \\ V_{\mathrm{Ca}} \\ V_{\mathrm{Cb}} \\ V_{\mathrm{Cc}} \\ V_0 \end{pmatrix} = \begin{bmatrix} 1 & -\frac{1}{2} & -\frac{1}{2} & 0 & -\frac{1}{2}\sqrt{3} & \frac{1}{2}\sqrt{3} & 0 \\ -\frac{1}{2} & 1 & -\frac{1}{2} & \frac{1}{2}\sqrt{3} & 0 & -\frac{1}{2}\sqrt{3} & 0 \\ -\frac{1}{2} & -\frac{1}{2} & 1 & -\frac{1}{2}\sqrt{3} & \frac{1}{2}\sqrt{3} & 0 & 0 \\ 0 & \frac{1}{2}\sqrt{3} & -\frac{1}{2}\sqrt{3} & 1 & -\frac{1}{2} & -\frac{1}{2} & 0 \\ -\frac{1}{2}\sqrt{3} & 0 & \frac{1}{2}\sqrt{3} & -\frac{1}{2} & 1 & -\frac{1}{2} & 0 \\ \frac{1}{2}\sqrt{3} & -\frac{1}{2}\sqrt{3} & 0 & -\frac{1}{2} & -\frac{1}{2} & 1 & 0 \\ 0 & 0 & 0 & 0 & 0 & 0 & 1 \end{bmatrix} \begin{pmatrix} V_{\mathrm{Da}} \\ V_{\mathrm{Db}} \\ V_{\mathrm{Dc}} \\ V_{\mathrm{Ca}} \\ V_{\mathrm{Cb}} \\ V_{\mathrm{Cc}} \\ V_0 \end{pmatrix} \tag{8.77}$$

We see from the cross-coupling matrix that V_0 has no cross-coupling with any of the other components; also is there no cross-coupling between Da and Ca, between Db and Cb, and between Dc and Cc. Another conclusion that can be drawn from the cross-coupling matrix is that there are only three combinations that form an orthogonal base: (V_0, Da, Ca), (V_0, Db, Cb), and (V_0, Dc, Cc). In the next section we will use the decomposition method introduced here to analyze voltage and current transients.

8.10.3.2 Practical Implementation The method introduced in the previous section has been implemented as follows:

- The transient is extracted in each of the three phases. Any of the methods discussed in Section 8.10.1 can be used for this.
- The seven modes are calculated from the extracted transients by using (8.75). This results in seven waveforms as a function of time. The zero-sequence component can be treated separately because it has no correlation with any of the other components. The other six components are correlated according to the cross-correlation matrix in (8.77). The assumption to be made is that one of the six components is dominating. In that case the dominating component will have the largest amplitude and its orthogonal component (Ca for Da, etc.) will have an amplitude close to zero.
- The transient is classified by its dominating component. The single-event characteristics introduced before can be calculated from the dominating component.

8.10.3.3 Measurement Examples The method introduced in the two previous sections has been applied to a number of measured transients. In all examples the transient is extracted by using a second-order notch filter centered at the nominal power system frequency (50 or 60 Hz) with a bandwidth of 30 Hz. The first example is the transient due to the energizing of one phase of a three-phase capacitor bank. The results are shown in Figure 8.66. In addition to to the seven components, the original waveform and the extracted transients for the three phases are shown. The method used for characterizing voltage dips, identifying the highest of six rms voltages, cannot be directly applied here. The amplitudes of Dc, Ca, and Cb are very similar: 108.6, 97.7, and 90.4 V, respectively. However, Cc clearly has the lowest amplitude. Also the six components show the same pattern as in the cross-coupling matrix:

$$U_{\mathrm{Da}} = U_{Db} = -\tfrac{1}{2} U_{\mathrm{DC}}$$
$$U_{\mathrm{Ca}} = -U_{\mathrm{Cb}}$$
$$U_{\mathrm{Cc}} = 0$$

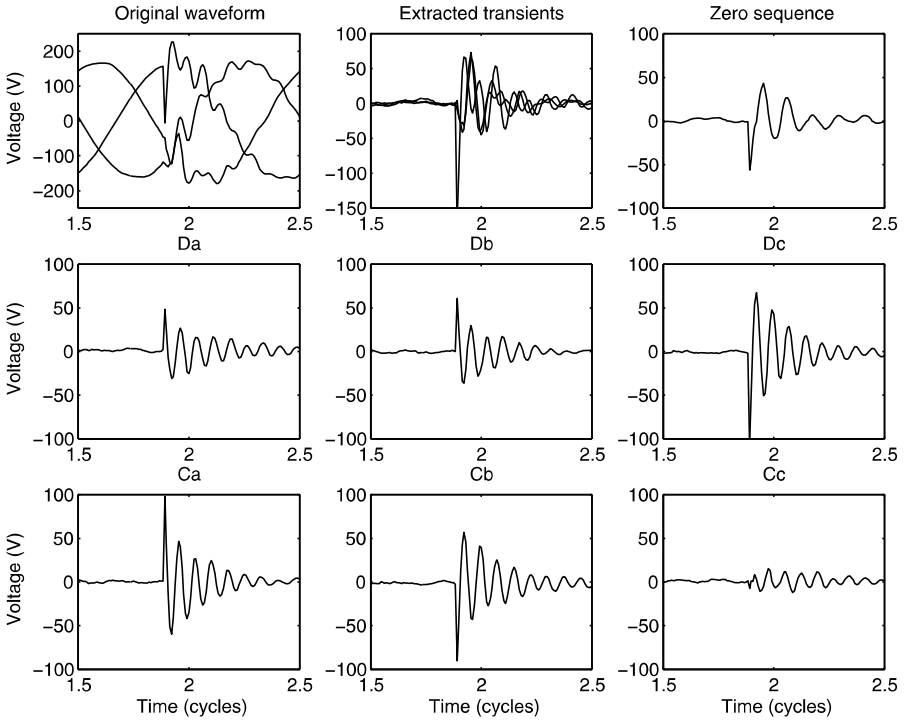


Figure 8.66 Original waveform, extracted transients in three phases, and seven components for measured transient: example 1.

Identifying this pattern is a good method to find the dominating component, which is Dc in this case. This event would thus be classified as a type Dc transient, with a peak-voltage of 108.6 V. The other characteristics, such as transient energy, oscillation frequency, and damping time constant, can be obtained in the same way as for a single-phase recording.

A second example is given in Figure 8.67; it is again the transient due to closing one phase of a three-phase capacitor bank. In this case the transient is classified as type Da: The pattern fits best with Da as dominating component. Note that the zero-sequence component is much higher than in the first example. Whereas the zero-sequence component was about half the dominating component in the first example, it is even somewhat higher than the dominating component in this case. Strictly speaking the zero-sequence component should be referred to as the dominating component in this case. But in the same way as for the classification of three-phase unbalanced voltage dips, the zero-sequence component will be treated separately. Another interesting observation from the plots is that V_{Da} and V_0 have the most smoothest waveform. Methods for extracting the oscillation frequency and time constant will be most successful when applied to these components.

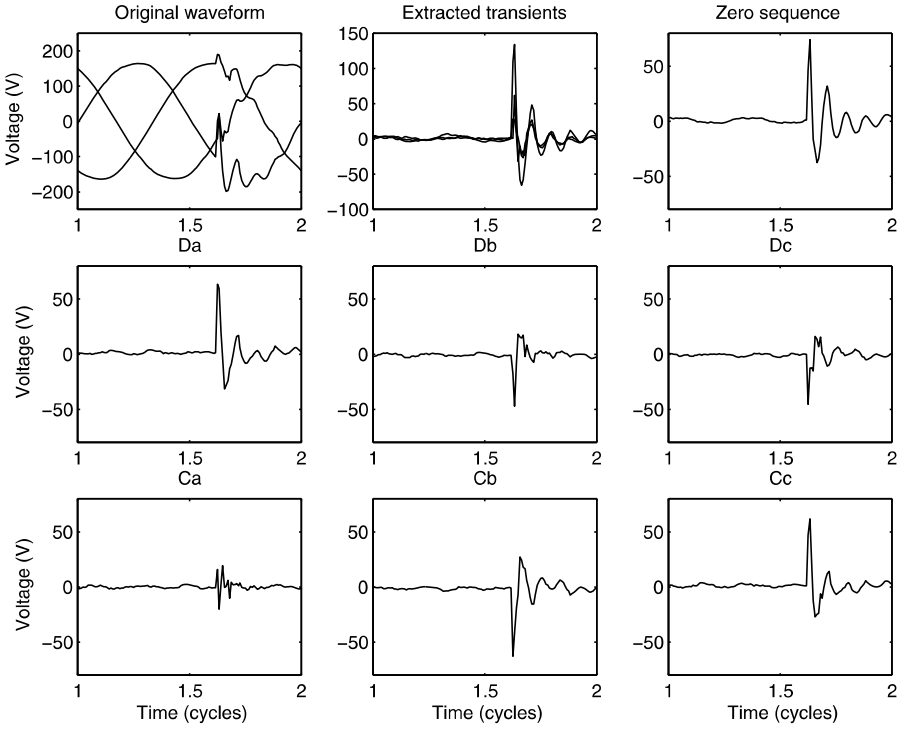


Figure 8.67 Original waveform, extracted transients in three phases, and seven components for measured transient: example 2.

Figure 8.68 shows the results of applying the method to a third example. This recording contains two transients, about one and a half cycle apart in time. The first transient is classified as a type Cc transient. A Cc transient corresponds to a switching action between phases *a* and *b*. With such a switching action one would not expect a zero-sequence component, in the same way as there is no zero-sequence component associated with type C voltage dips. However, closer inspection of the zero-sequence component shows that it is damped very quickly. It is probably due to a small difference in closing instant between phases *a* and *b*. The second transient is of type Dc and is probably caused by the closing of the third phase.

An example of a current transient is shown in Figure 8.69. The recording is obtained in a low-voltage network close to a medium-size industrial company. The transient is due to load switching on the customer premises. Based on the relation between the waveforms in the six components, the event is classified as a type Ca transient, being a switching action between phases *b* and *c*. The event is probably due to the switching of a drive. The current transient caused a voltage transient that was also classified as a type Ca transient.

Example 5 is the voltage transient due to synchronized capacitor energizing. As the aim of synchronized capacitor energizing is to limit the impact of the switching

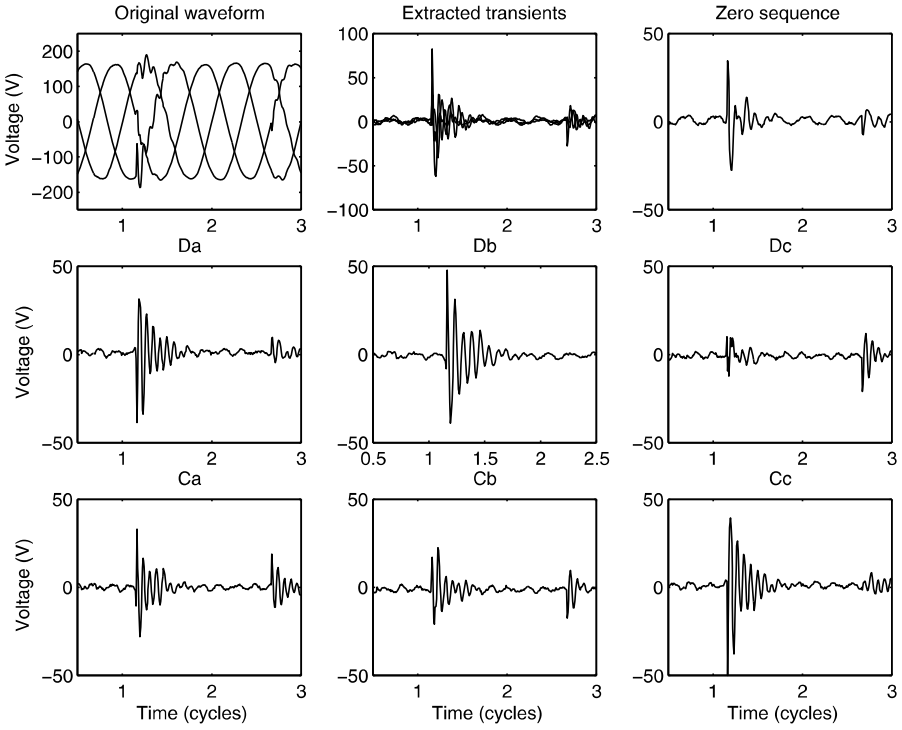


Figure 8.68 Original waveform, extracted transients in three phases, and seven components for measured transient: example 3.

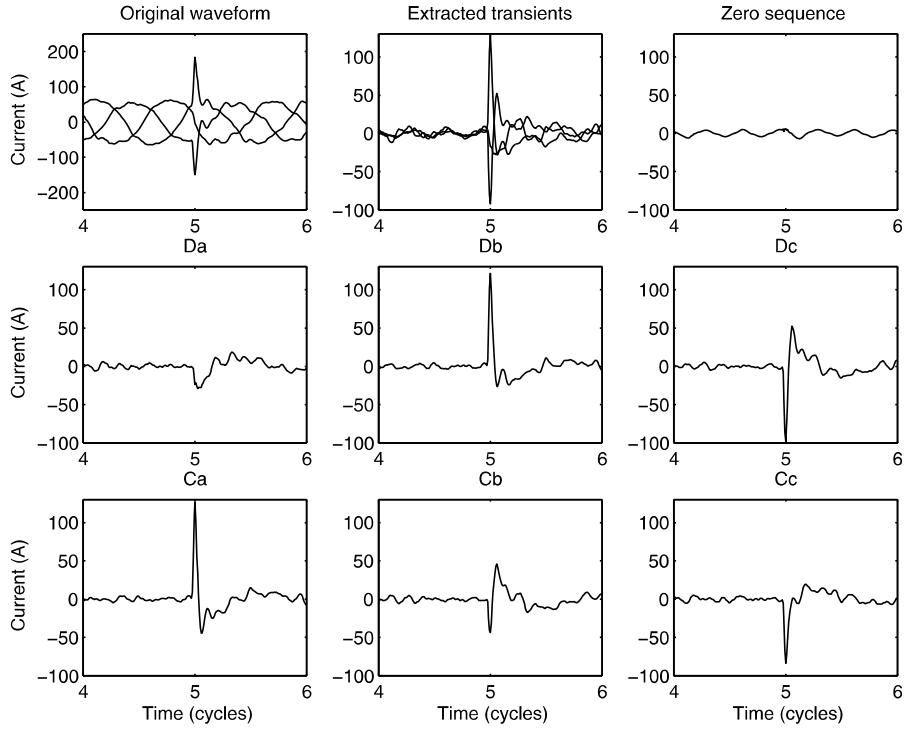


Figure 8.69 Original waveform, extracted transients in three phases, and seven components for measured transient: example 4.

action, the transient is of limited magnitude. It is however still large enough to be detected, and it should be noted that most switching actions went unnoticed even by the monitor. The transient shown is thus one of the more severe ones due to synchronized switching. Comparing this with the previous examples clearly shows the mitigating effect of synchronized switching. The results of applying the decomposition method are shown in Figure 8.70. At first impression the classification method cannot be applied to this transient. None of the six components are small, so that it is not possible to find the dominant component. However, a closer look at components Dc and Cc shows that Cc increases about one quarter-cycle earlier than Dc. This transient can thus be interpreted as the superposition of a type Cc transient and a type Dc transient, where the latter one starts one quarter-cycle after the first one. The capacitor bank in this case is star-connected but not grounded. Two phases are energizing at the zero crossing of their voltage difference, the third phase one quarter-cycle later. This corresponds with the Cc–Dc classification found. Note that Cc and Dc are the only components that show a smooth damped waveform; the other ones are all a superposition of two components. The oscillation frequency and other single-event indices should be extracted from Cc and Dc.

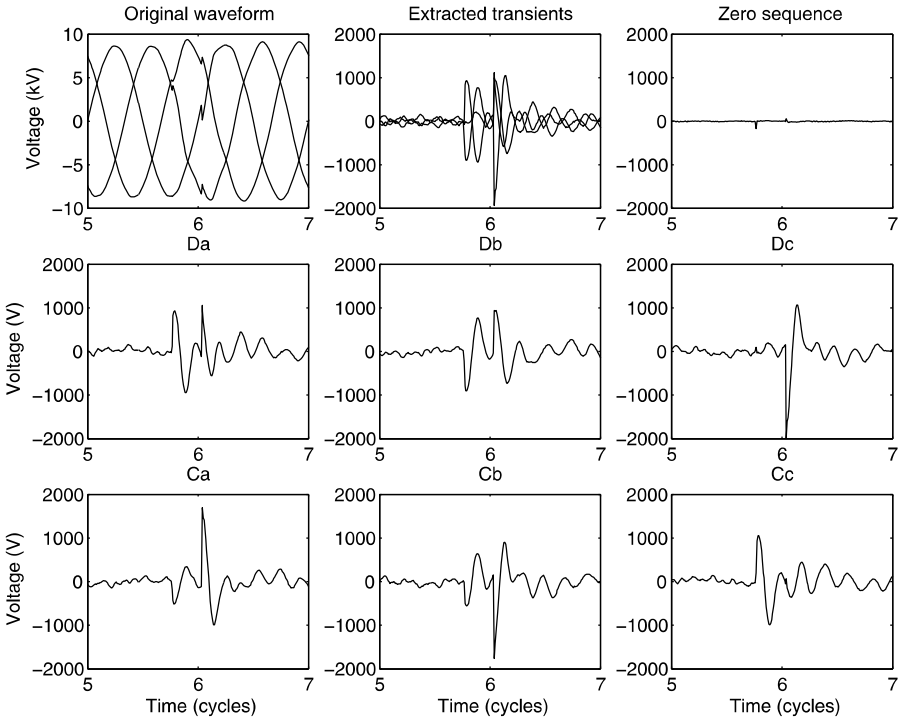


Figure 8.70 Original waveform, extracted transients in three phases, and seven components for measured transient: example 5.

8.10.3.4 Limitations of Method The methods for characterization and classification of transients in three-phase systems give a satisfactory result for most of the measured transients studied by the authors. The method is however based on the underlying assumption that no two switching actions occur at the same time. In the last example the two switching actions could still be distinguished because their time difference was somewhat more than one cycle of the transient oscillation. Any smaller difference in time will mean that the classification does not apply anymore. Such a transient should be labeled "nonclassified." The same holds when three switching actions occur shortly after each other.

The final example is such a nonclassifiable transient. Its component waveforms are shown in Figure 8.71. The origin of this transient is unknown, but it is probably due to restrike during capacitor deenergizing. Both Cc and Da are small compared to the other components, and both Dc and Ca are large. Thus both Dc and Ca could be classified as the dominant component. A close visual inspection of the waveforms for the six components shows Cb–Dc–Ca as a possible sequence, but the pattern is not very clear. An automatic pattern recognition algorithm may help in identifying such a sequence.

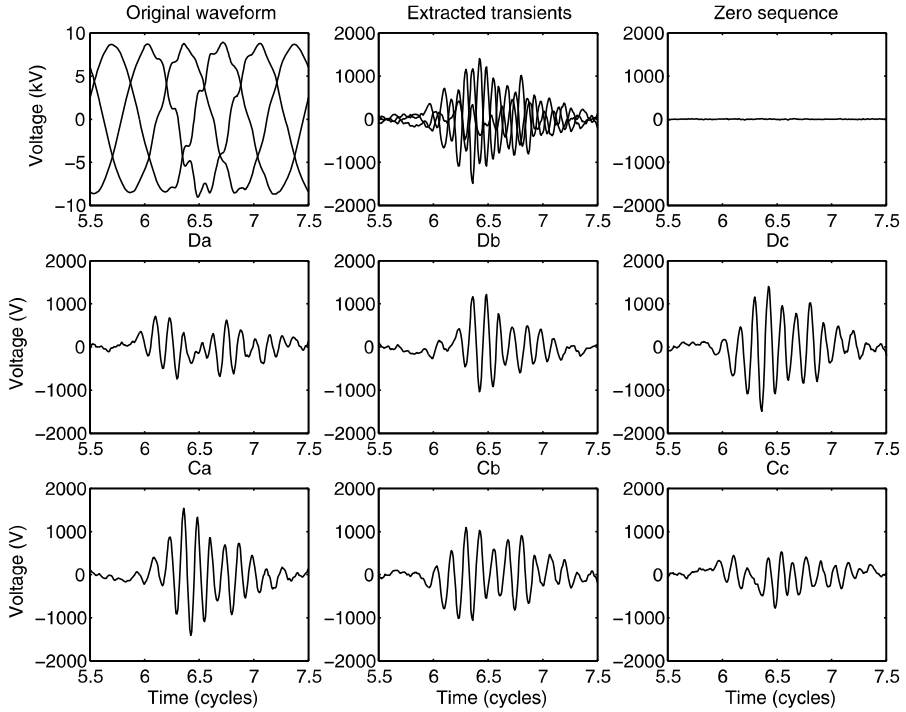


Figure 8.71 Original waveform, extracted transients in three phases, and seven components for measured transient: example 6.

There are a number of reasons why the classification algorithm works less well for transients than for voltage dips. At first there are the measurement problems: The harmonic distortion in the original waveform causes an error in the extracted transient. For small transients this may make the classification more difficult. The second cause of error is in the method used for extracting the transient. A change in fundamental component leads to an oscillation in the output of a notch filter that adds to the actual transient. When extracting the fundamental or the preevent waveform, the difference in fundamental adds to the transient.

Another source of error is in the model used for the system. The Clarke transform is based on a balanced model of the power system: All three phases are equal and the coupling between each pair of phases is equal. Whereas this is a reasonable model for fundamental frequency, it may no longer be acceptable for higher frequencies. The nonbalanced character of the system manifests itself as a coupling between the components; thus Ca, Da, and zero sequence are no longer fully decoupled. A method similar to the one presented here is used for selection of the faulted phase with some algorithms for traveling-wave-based protection [29, 295]. The coupling between the components is also mentioned in [29, 295] as making the selection more difficult. Note that the "superimposed components" mentioned in [295] correspond to our extracted transients.

The characterization method introduced here for transients on three-phase systems is comparable to the characterization of voltage dips under the assumption that the PN factor remain equal to 1 pu. This is an acceptable assumption for single switching events, either between phase and ground or between two phases. We saw however, when analyzing voltage dips in three phases, that a second characteristic is needed, the PN factor, to cover dips due to two-phase-to-ground and three-phase faults. Such an extension may also be needed for the characterization of transients.

8.10.4 Additional Information from Transients

Most of the discussion on the previous pages was directed toward characteristics of transients for statistical purposes and was thus aimed at quantifying the supply performance. When interested in the origin of a transient, information about its magnitude and duration is of limited value. Some other characteristics may provide additional information that may help in identifying the origin of the event.

8.10.4.1 Change in Steady-State Voltage or Current A transient is in many cases associated with a transition between two system states, for example, the energizing of a capacitor bank. This change in system state often also impacts the steady-state voltage or current magnitude and waveform. For a downstream switching event it is obvious that a change in steady-state current can be expected. But even an upstream switching event may cause a change in voltage magnitude. Capacitor energizing is the best example of a transient that affects the voltage magnitude and waveform. As shown in Section 2.2.3 the switching of a capacitor bank causes a change in voltage magnitude due to the injection of reactive power into the system. The switching of the capacitor bank may at the same time cause a significant change in the harmonic impedance and thus in the harmonic voltage distortion.

Consider as an example the voltage and current transient shown in Figure 6.70. This event is due to the synchronized energizing of a 6.6-Mvar capacitor bank just downstream of the measurement location. The three-phase characteristics of the voltages were shown in Figure 8.70 and the phase angle of the current versus time in Figure 8.22. The latter is especially interesting as it gives information about the underlying event without looking into the actual transient. The fact that the current advances 40° in phase angle indicates the presence of a large downstream source of reactive power. Some more characteristics are shown in Figure 8.72. The transient is associated with a rise in voltage of 3.4%, a rise in fifth-harmonic voltage from 0.5 to 1.2%, a rise in active power consumption by 4.5%, and a change in reactive power flow from 2.85 Mvar reactive to 3.95 Mvar capacitive. The rise in fundamental voltage is common for capacitor bank energizing. It is due to the injection of reactive power into the system (see Section 2.2.3). The rise in fifth-harmonic voltage is due to a harmonic resonance between the fifth and the sixth harmonics (see Section 2.5.5). If no other capacitance would be present at the substation, a 3.4% rise in voltage would correspond to a resonance frequency of 270 Hz. The additional capacitance, mainly due to underground cables, will even further reduce this frequency somewhat. Also note the significant rise in active power consumption.

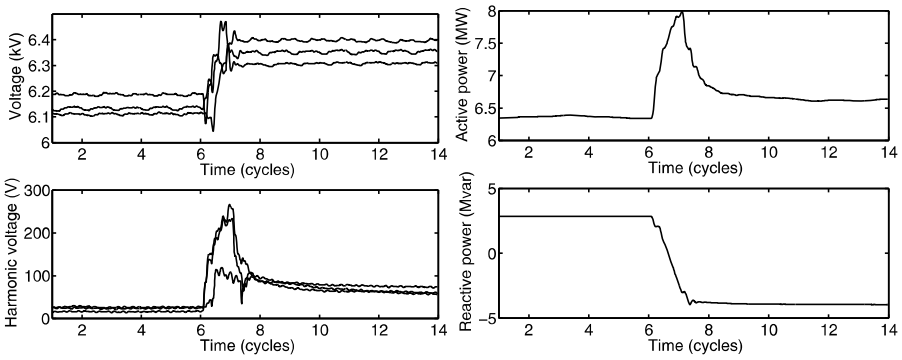


Figure 8.72 Changes in steady-state parameters for capacitor-energizing transient: rms voltage (upper left); fifth-harmonic voltage (lower left); active power (upper right); reactive power (lower right).

This is partly due to the losses in the capacitor bank, but mainly due to the voltage dependence of the load.

8.10.4.2 Frequency Spectrum Additional information may also be obtained from the spectral components of the transient. The dominant frequencies may be obtained by applying the discrete Fourier transform, as shown in Section 6.3, or alternatively from applying an ESPRIT or MUSIC method, as introduced in Section 3.5.2 and 3.5.3. The latter methods give more accurate estimates of the resonance frequency and even give estimates for the damping factors. In this case the spectrum only reveals harmonic components. From the step in voltage, the estimated resonance frequency is 270 Hz, which is too close to the fifth harmonic (250 Hz) to be detected by a simple DFT.

Figure 8.73 shows the voltage and current for a transient recorded at 132-kV subtransmission. The current measured is the total current through three 132/10-kV transformers. The current is lagging the voltage by 90°, which indicates a reactive load, in this case mainly formed by the three transformers. Plotting the product of the extracted voltage and current transient waveforms (the *transient power*, not shown here) shows that there is no net power flow outside the power system frequency. In the plot of the extracted voltage transient we see that the voltage contains a higher frequency component which is not present in the voltage. Only two currents were available, the transients parts of which are in phase, just like the transient part of the three voltages. The cause of this transient is not known, but from the measurements we can conclude that the source is upstream of the measurement location. The event is further associated with a 1% rise in positive-sequence voltage. We also see an increase in seventh-harmonic voltage (from 0.25 to 0.45%) and a minor increase in most of the other harmonic voltages (fifth harmonic rises from 0.66 to 0.78%). The latter may be associated with the change in harmonic currents, possibly related to the rise in voltage magnitude.

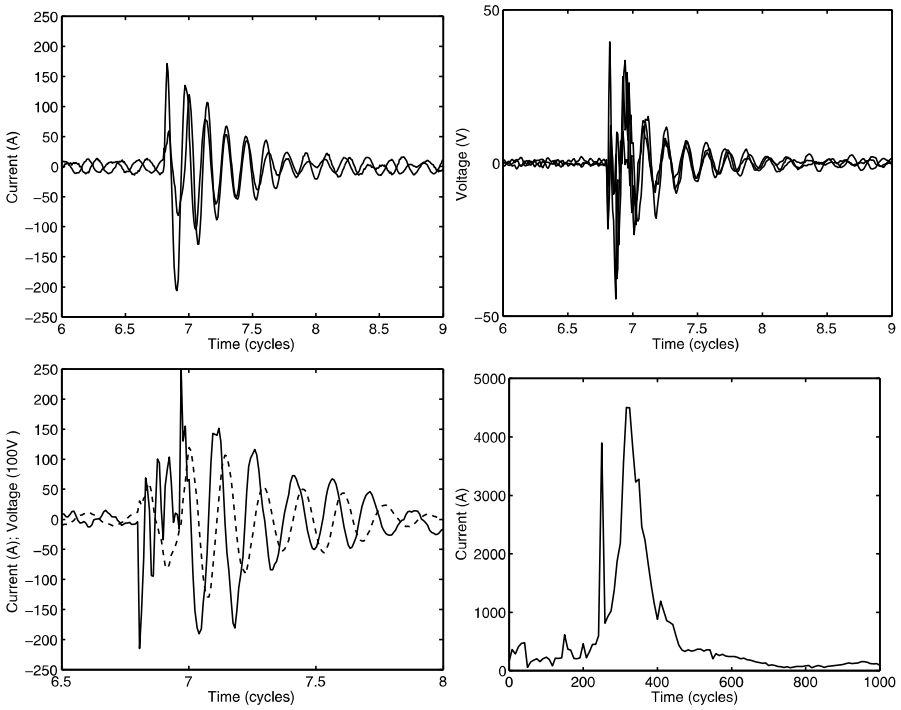


Figure 8.73 Additional information from transient recorded at 132 kV: current transient (top left); voltage transient (upper right); voltage and current transients (bottom left); spectrum of current transient (bottom right).

Both the rise in positive-sequence voltage and the change in harmonic spectrum point to capacitor energizing as the cause of the transient.

The spectrum of transient current (only one of the phases is shown) possesses a sharp peak around 250 Hz (due to the fifth harmonic) and a wider peak between 300 and 350 Hz. The latter is the resonance frequency of the capacitor bank being energized with the source impedance at the bank's location. As this is between the fifth- and seventh-harmonic voltages, it is understandable that both show a rise after the switching. We will come back to the voltage transients below. As the three voltage waveforms are available, it is recommended to first perform a component transformation.

8.10.4.3 Three-Phase Components The three-phase classification of transients, as introduced in the previous section, has been applied to the extracted voltage transients of this event. As only two currents were available, it was not possible to apply the method to the currents. The results are shown in Figure 8.74. The zero-sequence character, which was already visible in the previous figure, is better quantified now. The amplitudes of the seven components are similar, however, the non-zero-sequence components damp out in about one half-cycle whereas the

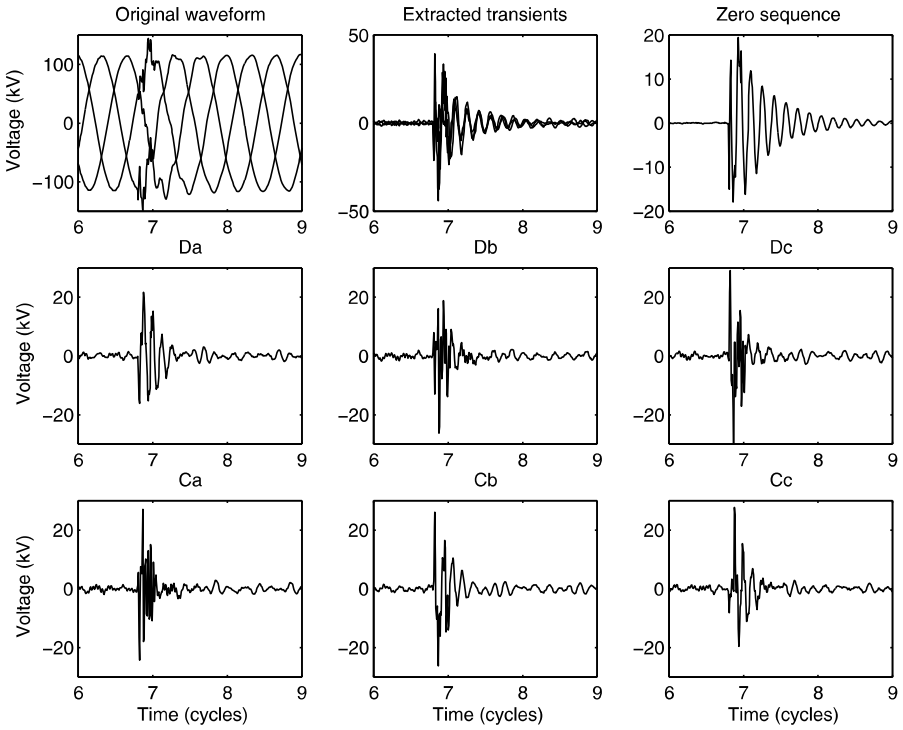


Figure 8.74 Three-phase characteristics of voltage transient shown in Figure 8.73.

zero-sequence component remains for more than one cycle. A close inspection of the different components shows that component Cc rises about 0.1 cycle after Dc. The initial transient is thus of Dc character (i.e., mainly in phase *c*); after the second phase is switched, the character of the transient becomes difficult to determine, in part because the dominant frequencies are relatively high compared to the sampling frequency being used.

The frequency spectra have been obtained for four of the components shown in Figure 8.74 by applying a DFT over a 10-cycle window. The resulting magnitude spectra for components V_0, Da, Cb, and Cc are shown in Figure 8.75. The zero-sequence component has a clear maximum near 320 Hz. The third-harmonic component at 150 Hz is also clearly visible. As shown in Section 2.5.3, the third-harmonic component has a mainly zero-sequence character in a balanced system. The spectra of the non-zero-sequence components have a completely different character: The fifth harmonic is dominating as well as a wide peak around 400 Hz which corresponds to the oscillations visible in Figure 8.74. A resonance frequency of 400 Hz would correspond with a voltage step of about 1.5%, which is close enough to the 1% step in positive-sequence voltage that is measured. Note that it is important to extract the three-phase components before the spectrum is obtained.

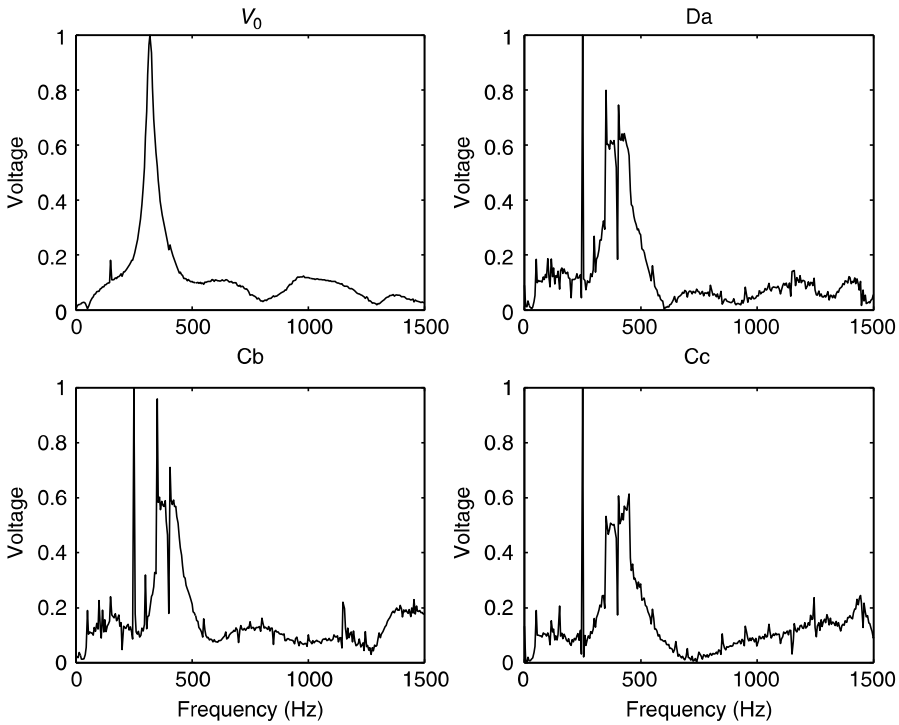


Figure 8.75 Frequency spectra for four of the three-phase components of voltage shown in Figure 8.73.

The oscillations in the zero-sequence component typically involve other capacitances and inductances than the ones associated with the step in voltage.

8.10.4.4 Voltage and Currents By comparing voltages and currents, information can be obtained about the direction of the transient, that is, whether the transient's origin is downstream or upstream of the measurement location. For a downstream origin, the current transient is the cause of the voltage transients, whereas the voltage transient causes the current transient for an upstream origin. With transients this is however not always obvious, especially when a capacitor bank is present downstream of the monitor location. Some examples of downstream and upstream events were shown earlier in this chapter as well as in Section 6.3.

8.10.4.5 Extracting Spectral Components Instead of using the DFT to obtain information on the spectral components in the transient, a model-based method can be used. A model-based method will result in a much more accurate estimate of the oscillation frequencies and will additionally give information on the initial phase and the damping time constants of the various spectral components. The ESPRIT and MUSIC methods, introduced in Section 3.5.3 can both be used.

For both methods it is essential that the power system component is removed. In [44] the ESPRIT method is used to decompose transient recordings in a number of damped sinusoids. Here we will apply this method to the components obtained from the three-phase classification.

The ESPRIT method introduced in [44] and Section 3.5.3 has been applied to the Clarke components as shown in Figures 8.74 and 8.75. In Figure 8.74 we see that the transients do not completely damp out due to the presence of waveform distortion in the original waveform. This waveform distortion has been removed by subtracting a periodic continuation from the last cycle of the recording. The last cycle has been chosen instead of the first cycle because the harmonic spectrum is typically different before and after a switching action leading to a transient. For the example discussed here, this resulted in a reduction of the remaining waveform distortion by about a factor of 5. This removal of the waveform distortion took place after the fundamental component was removed by the notch filter and before the Clarke components were calculated. Next the spectral components were estimated by using ESPRIT over a window starting at the initiation of the transient. The latter instant was obtained by visual inspection of the waveforms. The window length was taken equal to four cycles for the zero-sequence component. However, as the non-zero-sequence components are damped mostly within one cycle, the cycle length has been reduced to 1.5 cycles. The results for components V_0 and Da are shown in Figure 8.76. Both original and reconstructed transients are shown. The high-frequency part of the transient is not easy to reproduce in this case. The three phases involved in the transient close at different instants in time. With every closing instant a new high-frequency oscillation is generated. The occurrence of multiple transients starting at different time instants is not part of the model used in ESPRIT. By increasing the model order, it will be possible to obtain a reconstructed signal that is close to the original transient, but the resulting frequency components will not have physical meaning. In this example the model order was limited to 3 for V_0 and to 4 for Da.

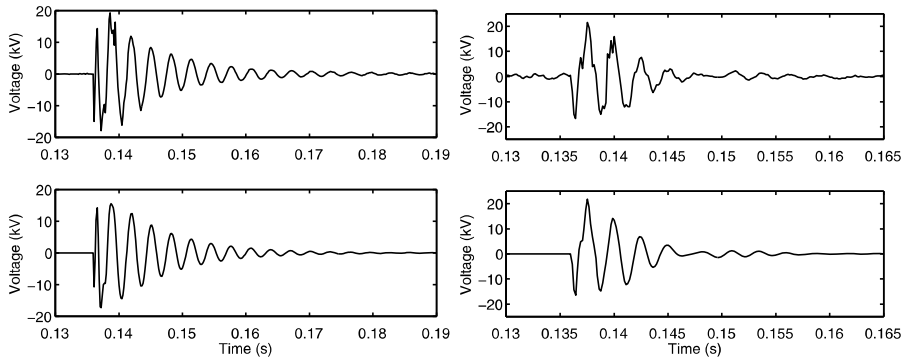


Figure 8.76 Original transients (top) and reconstructed transients (bottom) from frequency components estimated using ESPRIT: zero-sequence component V_0 (left); non-zero-sequence component Da (right).

The characteristics for the Clarke components are summarized in Table 8.23. Model order 3 has been used for V_0, model order 5 for Dc and Ca, and model order 4 for the other components. For V_0 the 320-Hz component is clearly the dominating one; it has a high initial magnitude and a long time constant. However, during the first few milliseconds the single-frequency model does not hold and additional frequencies are needed to describe the signal. Note that the 303-Hz component is almost in opposite phase with the 320-Hz component. The result is that the 320-Hz component is de facto not present during the first millisecond. Instead the 1-kHz component dominates there.

For Da the two dominating oscillations are 370 and 449 Hz. The other components either are of smaller magnitude or possess higher damping. For Cb we find that the 381-Hz component is dominating, whereas Cc has again two dominating components (366 and 451 Hz). A dominating frequency around 400 Hz is

TABLE 8.23 Characteristics for Clarke Components Estimated using ESPRIT

Component	Frequency (Hz)	Time Constant (ms)	Magnitude (kV)	Initial Phase (deg)
V_0	303	1.1	25.3	−138
	320	8.7	25.3	23
	1064	1.0	21.9	108
Da	127	4.6	4.7	−89
	370	5.4	16.7	−164
	449	4.5	15.5	54
	1315	1.7	8.5	−28
Db	424	4.0	19.1	−72
	538	0.5	68.4	92
	1257	1.1	57.3	−148
	1433	1.8	44.4	−8
Dc	89	0.8	60.1	66
	378	6.0	10.5	−14
	1226	1.0	55.5	87
	1394	2.0	43.1	−152
	1838	5.7	4.1	−13
Ca	417	0.9	26.2	161
	1190	1.3	38.4	−102
	1416	2.4	33.0	11
	1817	3.3	6.7	−165
	2326	1.6	8.3	−54
Cb	243	2.0	13.8	−26
	381	4.4	25.1	−10
	738	0.2	62.5	115
	1415	2.8	11.6	171
Cc	366	2.8	33.1	−135
	451	2.6	37.6	35
	1157	1.0	27.0	69
	1432	2.6	16.5	−164

TABLE 8.24 Characteristics for Four Clarke Components in First-Order Model

Component	Frequency (Hz)	Time Constant (ms)	Magnitude (kV)	Initial Phase (deg)
Da	402	7.3	16.7	134
Cb	397	5.9	17.7	−42
Cc	410	8.2	12.4	123
V_0	320	13.9	15.2	22

present for most non-zero-sequence components, except for Ca (the 417-Hz component is damped too fast to be of significance). Note also that a frequency component around 1.3 to 1.4 kHz is present with all non-zero-sequence components. By combining the information from all the components, we may conclude that two main frequencies are present in the transient: one around 400 Hz and another one around 1.3 to 1.4 kHz.

For comparison, Table 8.24 gives the same characteristics when a first-order model is assumed. The results are given for four of the seven Clarke components. For the other components, no suitable first-order model could be found. We may conclude from the results that the dominating frequency is 320 Hz for the zero-sequence component and around 400 Hz for the non-zero-sequence components.

It is important that the ESPRIT method is applied to a window in which the relevant parameters of the signal are stationary, that is, where the basic model is valid. In the basic model used the signal consists of the sum of a finite number of damped sinusoids. This requires that the starting and ending points of the transient are found. Here these have been chosen through visual inspection of the waveform. Alternative methods for automatic detection of such an interval may include using wavelets to find the corresponding singular points or a segmentation method that exploits Kalman filter residues. Choosing the starting point too early may result in the capture of traveling waves or the difference in switching instants in different phases. This may lead to unreliable results. Delaying the starting point will only reduce the signal-to-noise ratio but not the frequency and damping of the components. Further development of the method is needed before it can be used for automatic analysis of voltage and current transients.

8.11 SUMMARY AND CONCLUSIONS

The characterization of individual power quality events is generally a two-step process. The first step consists of the calculation of suitable characteristics versus time from the voltage or current waveforms. In the second step the characteristics versus time form a base for the calculation of single-event indices. The most commonly used characteristic versus time for voltage dips, swells, and interruptions is the one-cycle rms voltage (as defined in IEC 61000-4-30). It is shown that a sudden step in voltage magnitude at the start and end of the dip may lead to artifacts that could result in a wrong value for the single-event indices. A number of

alternative and additional characteristics are introduced in this chapter. Instead of the one-cycle rms voltage, the half-cycle rms voltage or the voltage amplitude (peak voltage) may be used to quantify the voltage magnitude. The half-cycle rms voltage gives a faster transition after a step in voltage but is also sensitive to even-harmonic distortion in the waveform. The peak voltage (half-cycle or one-cycle) could be an appropriate characteristic to quantify the impact of dips on electronic equipment. However, the method is rarely used. Some further discussion and additional standard development may be needed to propagate the use of the peak voltage instead of or in addition to the rms voltage.

Methods are discussed to extract the phase angle versus time of a voltage or current waveform. It is shown that accurate estimation of the frequency is needed and that the values obtained during transition segments are not reliable. Any automatic method for extracting phase-angle information from voltage dips thus requires a frequency estimation method as well as a method for detecting transition segments. Further development and implementation work are needed here.

Voltage-dip characteristics that consider the three-phase character of the power system are discussed in detail in this chapter. Two methods are discussed, both related to the three-phase classification of voltage dips as presented in Section 6.2.3. The symmetrical-component method is more accurate but somewhat more difficult to implement than the six-phase algorithm. Both methods result in a dip type plus three characteristics versus time. One of these characteristics, the characteristic voltage, is a generalized magnitude of the voltage that can be used to replace the rms voltage versus time as introduced for single-phase events. Currently, the IEC standards do not consider the three-phase character of the power system in the prescribed voltage-dip indices.

For voltage or current transients, the extracted transient is the most suitable characteristic versus time. Only for insulation-related problems is it appropriate to use the actual waveform. A number of methods have been introduced to obtain the extracted transient: subtracting the preevent steady-state waveform, subtracting the preevent fundamental voltage or current, the output of a high-pass filter, and the output of a notch filter centered at the power system frequency. Although each method has advantages and disadvantages, subtracting the preevent steady-state waveform and the notch filter appear the two most appropriate methods. Further development work is needed here, where a combination of these two methods (used in one of the examples in this chapter) should be investigated. No standard document discusses methods to extract the transient, which means that measurements obtained with different instruments may be difficult to compare.

Single-event indices are presented for voltage dips, swells, and interruptions and for voltage and current transients. The standard method prescribes the use of a duration for dips, swells, and interruptions; a residual voltage for voltage dips; and a maximum swell voltage for voltage swells. All these indices are obtained from the one-cycle rms voltage as a function of time. Single-event indices can also be obtained from the other characteristics versus time: the phase angle, the (three-phase) characteristic voltage, and the PN factor. A set of single-event indices is proposed based on these characteristics. The lowest characteristic voltage is a suitable alternative for the residual voltage in a three-phase system. A perceived

disadvantage of introducing additional indices is that this further increases the dimensionality of a voltage-dip event. The opposite tendency is to quantify the severity of an event by a single value. Two such indices are discussed here: the voltage-dip energy and the voltage-dip severity, where the voltage-dip severity has preferable properties. It should be clearly noted, however, that the authors are not propagating the use of single-index methods for anything other than as an intermediate step in the calculation of site and system indices, and even in that case it should be used with care. The use of a set of indices is preferred as this will provide additional information on the event and on the relation between event severity and equipment performance. Further work is needed to develop standard methods to calculate the additional indices. Further research is needed to establish relations between the different indices and equipment performance.

Also voltage and current transients are generally characterized by a magnitude and a duration. However, contrary to voltage dips, there is no clarity on the method used and different methods give significantly different results. The different methods are presented here, without giving an opinion about which method is preferred. It is seen as a task for standard-setting organizations to define a set of single-event indices for transients. There is simply not enough information available on the relation between transients and equipment performance to recommend the use of just one index. Such a set of well-defined indices could form a starting point for further study of equipment performance during transients.

A method has been introduced for the characterization of transients in a three-phase system. The method is based on the Clarke transform and results in seven components. It is shown that the method is a generalization of the method for characterization of three-phase unbalanced voltage dips. In a three-phase system the single-event indices should be obtained from the Clarke components. To understand this method better, it should be applied to a sufficient number of simulated and measured transients.

The material on transients presented in this chapter is limited in at least two aspects. The frequency range has been limited to a few kilohertz due to the availability of measurement data. However, most of the methods presented can be applied to higher frequency ranges as well. The other limitation is that we only consider phase-to-ground and phase-to-phase voltages. With transient measurements the neutral-to-ground voltage is as important to equipment performance as the phase voltages. Systematic research on this subject has not even started but will be important in order to understand voltage transients.

Another subject on which a wide research effort is needed concerns the extraction of additional information from event recordings. Such information can be important when deciding on mitigation methods against power quality disturbances. However, event recordings also provide useful information on system performance that often cannot be obtained in any other way. A set of expert-system rules are presented that have been successfully used in an automatic system for classification of voltage-dip recordings based on the origin of the event. Whereas the rules are rather well understood for voltage dips, such a system for transients is still far from complete. Some general considerations are presented here, including a method to identify the main frequency components from the extracted waveform.